

**Camp Security Geophysical Survey 2018:
A Report For The Friends of Camp Security (FOCS)**

PREPARED BY

*Department of Geography-Earth Science
Shippensburg University*

Dr. Sean Cornell

Dr. Paul Marr

Dr. Joseph Zume

ASSISTED BY

Jacob Percey

Thomas Vento

Nathaniel Fricke

Cameron Weiser

IPSSP Grant # 2860

Final Report Submitted: July 1, 2018

TABLE OF CONTENTS

Introduction	3
Camp Security Physiography/Geology/Hydrology/Soils	5
Physiography	5
Geology	5
Hydrology	8
Soils	10
Methods	11
Site Preparation	12
Topographic Mapping	12
Grid Layout	13
GPR	17
EM	23
Results and Interpretation	24
GPR Results	24
EM Results	29
Anomalies of Interest	32
Schultz Block	32
Wiest Block	32
Anomaly Ranking	32
Recommendations and Conclusions	34
Acknowledgements	39
References	40
Appendix 0	42
Appendix 1	43
Appendix 2	44
Appendix 3	46

LIST OF FIGURES AND TABLES

Figures		
1	Camp Security, near York, PA	1
2	Overview of the Camp Security study area showing previous investigations	1
3	Locations of the Wiest and Schultz blocks	4
4	Local geologic units	5
5	Geologic unit examples as they are found in the Schultz block	7
6	Topographic, geologic and hydrologic features of the Piedmont Physiographic Province	8
7	View south showing one of several small disconnected springs	9
8	Soils within the Camp Security protected area	10
9	Photograph taken on 12/11/2017 from the SW corner of the Wiest block	11
10	Photographs of volunteers beginning to open the hedgerow	12
11	Photograph of GPS with external antenna used in this study	12
12	Camp Security 2018 benchmark locations	13
13	Map showing N, E, Z grid points for Wiest block survey	14
14	Volunteers assisting in set-up of the southern boundary of the Wiest block	14
15	Photograph facing south (uphill) on the Wiest block	15
16	Photograph of the Schultz block looking northward toward the Schultz farm	15
17	Overview map that shows all grids for the survey	16
18	Graphic demonstrating basic equipment set-up and data acquisition theory	18
19	GPR set-up showing 500 Mhz antenna with triggering wheel attached	19
20	Radargrams from Schultz Block	19
21	Schematic cross-section of subsurface intervals investigated with GPR in this study	20
22	Overview of the basic data processing work flow used in this study	21
23	Raw and processed radargram collected with 500 MHz X3M	22
24	Colorized map-view output options for a test run of the Wiest block data	23
25	Data collection using the GSSI EMP Profiler unit	24
26	GPR transect lines for the 3 high resolution survey grids	25
27	Radargram export from RadExplorer after filters were applied	26
28	GPRSlice map-view time slices from the surface downward 3_15_18 Schultz block	27
29	GPRSlice map-view time slices from the surface downward 3_13_18 Wiest block	28
30	GPRSlice map-view time slices from the surface downward 3_15_18 Wiest block	28
31	Anomaly of Interest (AOI) from Wiest block (WB1-1)	29
32	EM conductivity results from the Wiest block grids	30
33	EM conductivity results from the Schultz block grid	31
34	Shultz block GPR anomalies of interest	33
35	Wiest block GPR anomalies of interest	34
36	Wiest block EM anomalies of interest	35
37	Anomalies of interest overview	36
Tables		
1	Profile names and dates	16
2	Ground Vision parameterization	18
3	Anomaly ranks and locations	33

INTRODUCTION

Camp Security was a prison camp used during the American Revolutionary War to house British troops captured at Saratoga, New York in 1777, as well as prisoners captured at Yorktown in 1781. Lt. William Scott of the York County Militia was instructed to find a suitable location for the camp that was well wooded and had access to water. The camp was constructed in 1781 on a farm belonging to David Brubaker, approximately 4 miles east of the town of York, Pennsylvania (Figure 1). The camp consisted of two separate sites: Camp Security where Yorktown prisoners were housed within a stockade and Camp Indulgence, a hut village nearby. Prisoners of war were held at the camp until May, 1783 and the war was formally ended with the signing of the Treaty of Paris in September of that year. In total, the camp was occupied for less than two years. After the war the land was returned to David Brubaker and the camp

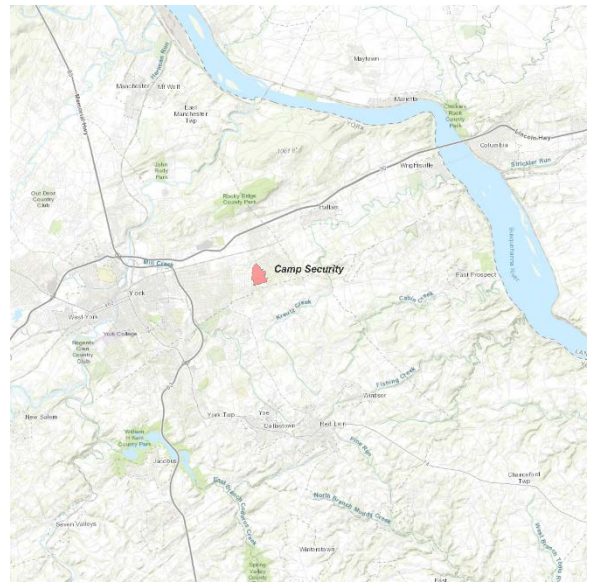


Figure 1. Camp Security, near York, PA.

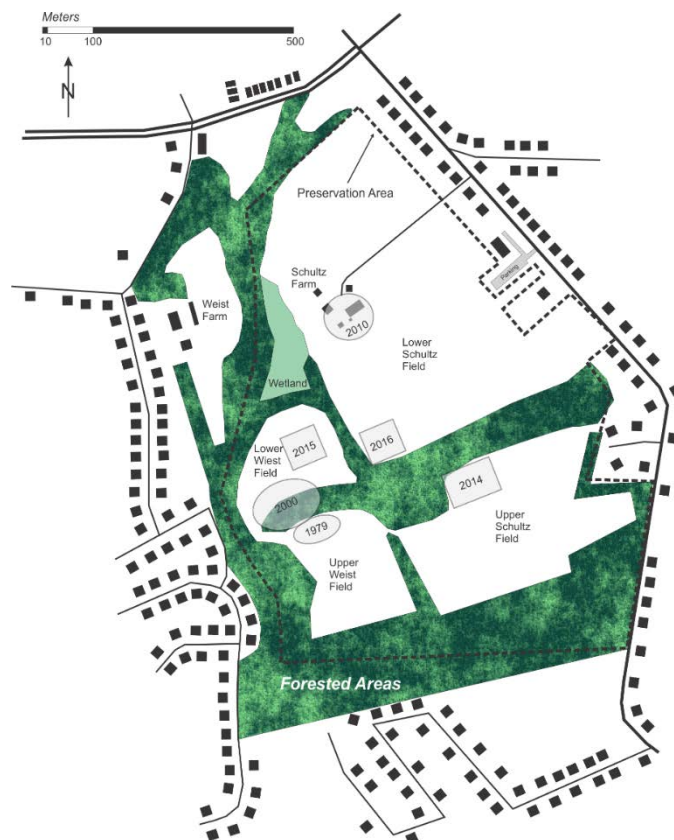


Figure 2. Overview of the Camp Security study area showing previous investigations. Buildings are not to scale.

began to deteriorate. The huts and stockades were pulled down and the wood used in other construction, with the land eventually reverting back to farming. By the early 1900s the little remained of the site, save for a few fence railing and foundation stones. By the late 1900s, in his *History of York County Pennsylvania* (1907) George Prowell's prediction that "*unless it (Camp Security) is marked, the exact site will be known to future generations only by tradition*" had come true and all traces of the camp were gone.

Systematic efforts to rediscover the locations of Camps Security and Indulgence began with an excavation in 1979. These efforts focused on the western part of the upper field of the Weist tract (Figure 2). While extant documentary sources gave little information on the specific location of the camp and local lore often gave conflicting information concerning the camp's location, sufficient surface artifacts were found during the 1979 excavation to warrant further exploration. In 2000 a surface survey was conducted just north of the 1979 excavations, extending from the

upper Wiest tract, through the wooded slope, and into the southern section of the lower Wiest tract. In 2010 a large number of test pits were excavated in the immediate vicinity of the Schultz farmhouse. Larger excavations focused on the upper Schultz tract (2014), the lower Wiest tract (2015), and the lower Schultz tract (2016). Although in each of these efforts Revolutionary War era artifacts have been recovered, evidence of the location of the camp remains elusive.

Several forms of sub-surface sensing had been used previously in the archaeological investigations at Camp Security (e.g. metal detectors, gradiometer). While these systems are capable of detecting subsurface anomalies (disturbances in the natural soils depositional processes) their resolving power—ability to detect small variations—is somewhat limited. The systems which have the best capabilities for detecting near-surface archaeologically important features are ground penetrating radar (GPR) and electromagnetic induction (EM). Both systems are able to use high frequency electromagnetic waves to finely resolve the shallow subsurface environment. In an effort to help determine the location of the camp, the Department of Geography-Earth Science at Shippensburg University was contracted to use both GPR and EM to examine two large sections (hereafter referred to as Wiest block and Schultz block, See Figure 3) of the Camp Security Preservation Area for subsurface anomalies. Any anomalies found would be ranked in terms of their likelihood of being associated with the camp and targeted for future archaeological investigations.

Our analyses used a multi-pronged approach which we feel not only increased our chances of fixing the camp’s location, but will also organize all of the data from the current and previous investigations in a highly useable format. Our previous experience has shown that data organization and ease of accessibility are extremely important—but often overlooked--component when examining spatial data. Our goals therefore were twofold: 1). to develop a detailed map showing all anomalies found during our subsurface imaging investigations along with ranks as to their likelihood of being associated with the camp, and 2). create a seamless and integrated spatial database for future analyses and mapping.

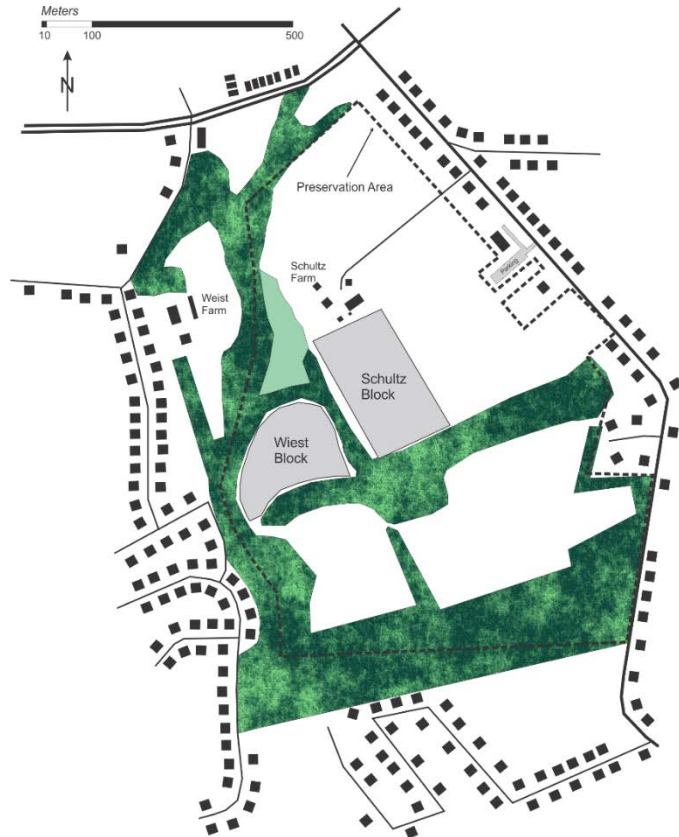


Figure 3. Locations of the Wiest and Schultz blocks.

CAMP SECURITY PHYSIOGRAPHY/GEOLOGY/HYDROLOGY/SOILS

Physiography

The Camp Security project area in Springettsbury Township, York County, Pa is located in the Piedmont province on the boundary of the Piedmont Uplands and Piedmont Lowland sections. The Piedmont Upland section extends from southern York County across the southeastern part of the state to southern Bucks County north of Philadelphia, and is bounded on the north by the Piedmont Lowland and Gettysburg-Newark Lowland sections and on the southeast by the Atlantic Coastal Plain province. Upland elevations on the schists are typically 400 to 500 feet, but elevations in southern York County are as high as 1,000 feet. Locally, there is as much as 100 to 200 feet of relief between the schists and adjacent rock types. Relief on the schists in southern York and Lancaster Counties is as much as 300 to 450 feet.

The Piedmont Lowland areas are underlain predominantly by Cambrian and Ordovician carbonates, but Precambrian-Lower Cambrian quartzites and Ordovician shale are also present. The carbonates underlie the lowland areas, typically at elevations of 300 to 400 feet, but are lower or higher in elevation depending upon their distance from the Susquehanna River. As in the Great Valley, the shale terrain lies about 50 to 100 feet above the carbonates, and the Cambrian sandstones produce ridges as much 400 to 500 feet above the adjacent carbonates. Subdued karst topography is common on the carbonates (Potter 1999).

The Piedmont Upland physiographic province is generally underlain by igneous and metamorphic rocks of Precambrian to Early Paleozoic age (Berg et al. 1980). Work by Wagner and Sroggi (1987) suggests that this area was a collision site between a magmatic arc and the Precambrian North American continent along an east-dipping subduction zone. Rocks of the Piedmont Upland have been repeatedly metamorphosed, intruded, folded and thrust faulted over time (Stose and Jonas 1923). Earlier work by Lyttle and Epstein (1987) indicates that the Piedmont may be divided into northern and southern sections at a contact between the Albite-Chlorite Schist and the Oligoclase-Mica Schist of the Wissahickon Formation. This contact may represent an important suture that joined the two distinctly different terranes probably before the Proterozoic or earliest Paleozoic (Lyttle and Epstein 1987).

Geology

The Chickies Formation (Cch) is composed of three lithologies – Hellam Conglomerate, Chickies Quartzite, and Chickies Slate (Figure 4; Bascom and Stose 1938). The Hellam Conglomerate is the basal member, which is made up of pebbly arkosic quartzite to coarse quartz feldspar- and quartz-pebble conglomerate grading into conglomeratic quartzite (Stose and Jonas 1939). It is notable that the Hellam Conglomerate is present everywhere the Chickies Formation has been mapped (Low et al. 2002). The Chickies Quartzite is medium-grained, massive, and well-bedded vitreous white quartzite with clear quartz grains and fine-grained, thin-bedded sericitic quartz schist (Low et al. 2002). In the study area *skolithos* tubes (fossilized vertical marine burrows) are relatively common; however, cross-bedding may only be locally observed. Quartz veins are often present between and cross-cutting



Figure 4. Local geologic units.

within bedding planes (Low et al. 2002). The Chickies Slate consists of black slate, green phyllite and thin-bedded quartzite (Stose and Stose 1944). In total, the Chickies formation ranges from 430 feet – 1,300 feet from south to north (Lyttle and Epstein 1987). Adams and Goodwin (1975) suggest that the Chickies Formation was deposited in braided streams and in the littoral zone along the coastal margin. The Chickies Formation unconformably overlies or is in contact with faults associated with granitic, plutonic, or other Precambrian rocks of the Piedmont Upland (Low et al. 2002). It conformably underlies the Harpers and Antietam formations, which are often undivided in the region.

The Antietam and Harpers formations (undivided, Cah) is a fine to medium-grained, light gray to grayish-green quartzite and quartz schist that often weathers to a buff or rusty brown. In York County, Stose and Jonas (1939) described three members to the Cah – lower fine-grained member streaked with argillaceous matter, a middle more resistant coarser-grained member, and an upper member consisting of granular, ferruginous laminated quartzite beds that produce porous rusty blocks by the solution of calcareous material. In general, the Cah is highly resistant to weathering and forms hills of medium to high relief with moderately steep and stable slopes (Low et al. 2002). Faulting, shearing and tight folds are fairly common and joints are moderately developed and wide-spread. The thickness of the unit ranges from >100 feet in York County to 450 feet in Chester County (Stose and Jonas 1939, Lyttle and Epton 1987). Kauffman and Frey (1979) interpreted the Cah as having been deposited in barrier island environments fronting the Cambrian continent as sea-level rose. In terms of stratigraphy, the Cah conformably overlies the Harpers Formation, where they are divided, and then grades into the Vintage Formation (Stose and Jonas 1939). Due to the presence of trilobite fossils, the Cah has been assigned a Lower Cambrian age (Walcott 1896).

The Vintage Formation (Cv) is mostly fine to medium-grained mottled or finely banded gray to blue thick to massive-bedded dolomite. In general, limestone is common in the upper part of Cv; however, fine-grained white, argillaceous to sandy dolomite or marble commonly represents the lower parts (Low et al. 2002). In York County, Cv grades out of the ferruginous and calcareous sandstone beds present at the top of the underlying Antietam Formation. (Stose and Jonas 1939). It often crops out as numerous but scattered, folded and faulted rocks that border the hills of the Antietam, Kinzers and Conestoga formations (Low et al. 2002). The Cv is conformably overlain by the Kinzers formation and is considered to be time-equivalent to the lower part of the Tomstown Formation of the Great Valley. The Cv is moderately resistant to weathering and forms valleys with slopes of low to moderate relief (Low et al. 2002). Over time, chemical weathering has created a highly irregular contact between the regolith (subsoil) and bedrock forming some shallow bedrock pinnacles as well as solution openings along existing joints and fractures (Geyer and Wilshusen 1982). Thickness of the Cv is variable with maximum thickness estimates ranging from 350 to 550 feet in Lancaster County to about 1,000 feet in York County (Stose and Jonas 1939). Taylor and Durika (1990) interpreted the Cv as turbidite deposits derived from carbonate platforms. As shown in Figure 4, the target area of this study are underlain primarily by Antietam/Harpers in the southern portion of the investigation area and the Vintage carbonates in the northern area.

The Kinzers Formation (Ck) is separated into three members in York County, PA – a basal shale member, a middle limestone, and an upper sandy limestone (Stose and Jonas 1939). The basal shale member is a black to dark gray or dark brown shale to greenish phyllite, which ranges in thickness from 42 to 200 feet in York County, PA (Ganis and Hopkins 1990). The middle limestone member is generally thick-bedded to massive, light to dark gray, finely crystalline and often contains argillaceous masses. Also present are beds of partially altered dolomite, marble, and structures that resemble Archeocyathid reefs (Stose and Jonas 1939). Primary sedimentary features include oolites, burrows, indistinct reef structures, desiccation features, bioclastic lag deposits, and metaconglomerates. Megabreccias have also been reported. Thickness of this unit ranges from 1,000 feet to 1,200 feet in York County (Ganis and Hopkins 1990). The upper member in York County, PA is a fine quartz-rich limestone banded with dark

argillaceous layers, which weathers to a buff tan color and alternates with darker porous fine sandstones and dark shales (Ganis and Hopkins 1990). Thickness of this upper unit ranges from 0 to 100 feet in York County (Ganis and Hopkins 1990). In York County, it is moderately resistant to weathering but the middle limestone member often forms narrow valleys between a pair of low ridges which are supported by the more resistant basal shale unit and the upper sandstone unit (Stose and Jonas 1939). Joint and cleavage planes are moderately developed, very common and usually opened (Geyer and Wilshausen 1982). Stose and Jonas (1939) interpreted the Ck as off-shelf, deeper water environments. According to Taylor and Durika (1990), the York member represents a foreslope facies formed during significant sea level rise in the late Cambrian. The conglomerates and megabreccias are thought to be the result of massive submarine landslides. The Ck is gradationally overlain by the Ledger Formation and is considered time equivalent to the lower part of the Tomstown Formation of the Great Valley (Stose and Jonas 1939).

The Conestoga Formation (OCc) is the highest stratigraphic unit in the study area. It has been divided into an upper and lower limestone member (Low et al. 2002). The upper member consists of medium bluish-gray, fine to coarse-grained, graphitic or micaceous limestone with argillaceous, shaley partings. The lower member consists of gray to blue, coarse-grained, thin to thick-bedded limestone, argillaceous limestone and dolomite. The bottom of the OCc is identifiable from limestone conglomerate beds, which have clasts that range in size from pebbles to boulders 30 feet across (Low et al. 2002). In some places, coarsely crystalline, silty and sandy limestones also occur and are sometimes interbedded with conglomerates. Lyttle and Epstein (1987) noted that in the Chester Valley, the contact between the upper and lower parts is the locus of considerable faulting, which may contain slivers of the Octoraro Phyllite. In general, the OCc is moderately resistant to weathering and forms rolling hills and valleys. Joints of the OCc are poorly formed, but are moderately abundant and tend to be open (Geyer and Wilshusen 1982). Thickness of the regolith is highly variable with fairly common bedrock pinnacles present (Geyer and Wilshusen 1982). While the top of the OCc is representative of a tectonic contact, the base of the OCc has long been considered, at least in some areas, an unconformity (Jonas and Stose

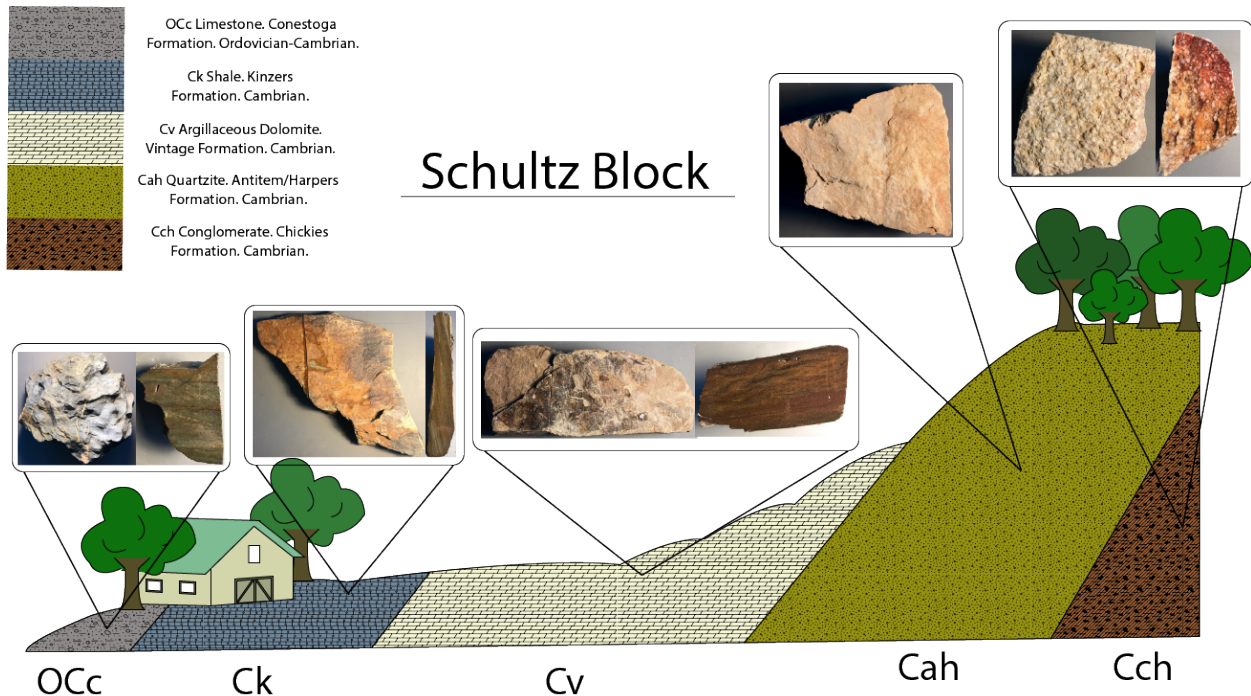


Figure 5. Geologic unit examples as they are found in the Schultz block.

1930). MacLachlan (1990) interpreted the OCc to represent slope deposits that contain proximal megabreccia to thin distal turbidites with dark phyllitic partings. Taylor and Durika (1990) interpreted the upper limestone member to represent proximal toe-of-slope debris flow deposits from the adjacent shelf margin. In general, the exact thickness of the OCc is unknown; however, Lloyd and Growitz (1977) estimated a thickness of 300 to 1,000 feet in York County. Representative rock samples (from the five units in the study area) collected during surveys can be seen in Figure 5. Most samples were collected as float specimens from the surface but recent excavation for the sanitary sewer lines on the western edge of the study area have exposed portions of the Antietam and Vintage. Lithologies of the bedrock and their representative weathering profile, porosity, permeability and fracture/joint patterns ultimately influenced the flow of surface and subsurface water. Relative to this study, the low porosity/permeability of the Antietam/Harpers (Cah) interval and the relatively higher porosity/permeability and open fractures within the Vintage (Cv) carbonates have undoubtedly contributed to the development of springs which not only provide water to the farm house on the Schultz block today, but were likely to have been important features during the construction and habitation of the forts.

Hydrology

The Piedmont Upland receives nearly uniform precipitation throughout the year; however, much of the recharge to ground water takes place from late fall to early spring (Low et al. 2002). During the remainder of the year, rapid plant growth, high evapotranspiration rates, and soil-moisture deficits greatly reduce the amount of recharge that reaches the ground-water system (Low et al. 2002). Much of the precipitation returns to the atmosphere or reaches streams as overland flow or runoff. The precipitation that is not lost to evapotranspiration, soil saturation, or overland runoff infiltrates into the regolith and the underlying bedrock. After reaching the saturated zone, ground water moves from areas of high hydraulic head to areas of lower hydraulic head and eventually returns to the land surface through wells, springs, or streams (Low et al. 2002). Ground water discharged to streams as base flow is important to maintain adequate streamflow and to dilute effluents discharged during periods of little precipitation. Lloyd and Growitz (1977) estimated that in central and southern York County about two-thirds of the water that constitutes streamflow is ground water.

A previous study

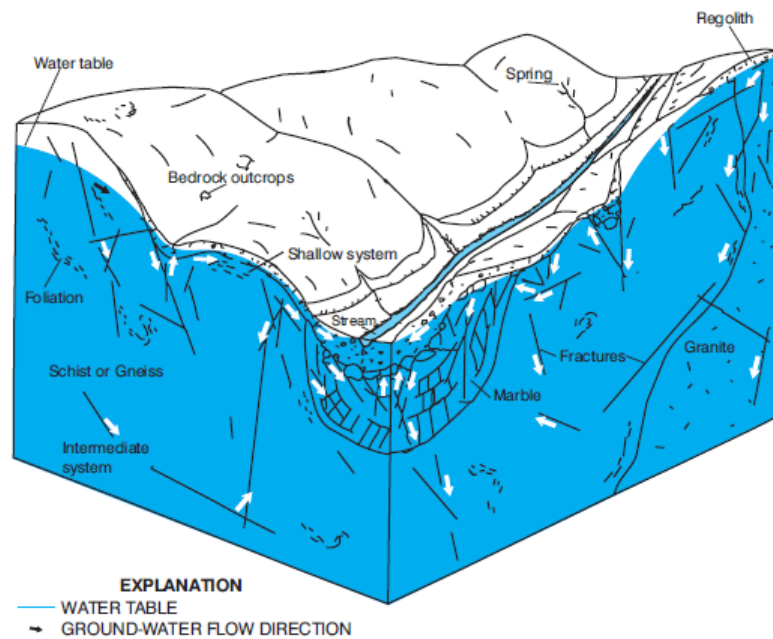


Figure 6. Illustration displaying the topographic, geologic and hydrologic features of the Piedmont Physiographic Province, Piedmont Upland Section. Taken from Low et al. (2002).

by Gerhart and Lazorchick (1988) using annual precipitation, base flow, and lithologies determined that 28% of annual precipitation became ground-water recharge for Paleozoic sedimentary rocks and 22% of annual precipitation recharged ground water in the crystalline rocks. The most important regional bedrock aquifer in the Piedmont Upland is the Oligoclase-Mica Schist. It underlies much of the entire Piedmont Upland, including the more populated areas. Important, highly productive, local bedrock aquifers include the Cockeysville Marble and the Peach Bottom Slate and Cardiff Conglomerate. Less productive units include the Plutonic Rocks and Albite-Chlorite Schist; the least productive unit is the Marburg Schist. Ground-water flow in the Piedmont Upland is dominated by local flow with ridges or hilltops commonly serving as water-table divides (Figure 6).



Figure 7: View south showing one of several small disconnected springs located between the lower Wiest and Schultz fields and below the inferred location of the Camp Indulgence area. One or more of these springs were likely candidates for use during the operational life of Camp Security.

According to LeGrand (1988), the small, numerous, ground-water systems that comprise local flow closely correspond to small surface-water drainage systems in which a perennial stream is present. In the study area, surface water flows move from the southeast to the northwest both at the surface as well as through the subsurface. A key hydrologic feature and an important source of water on the tract are small ephemeral springs. One particular spring is pictured in Figure 7 which shows groundwater discharging to a surface seep. In the background a more substantial gully is present and conveys combined surface water during storm events and groundwater during base flow. Another spring is located just north of this site and has a spring house built over it as the water is captured and piped underground to the Shultz Farm. Ultimately stream flows are directed toward Kreuz Creek and one ephemeral tributary losing stream which flows north between the two study area blocks.

Soils

Within the study area all of the soils are silt loams (Figure 8). The depth of the soils averages about 9in, with an average depth to bedrock of 5ft (60in) or greater—with the exception of Mount Airy soils where the depth to bedrock ranges from 20 to 40in. These in particular are present in the southern portion of the study area. Overall, the soils tend to be relatively well-drained, with moderate water capacity and medium runoff. Most are quite suitable for cropping, pasture, or forest. All tend to be dark brown and friable. The specific soil characteristics are below.

Chester silt loam (CeB: 3-8% slope and CeC: 8-15% slope) - Dark brown friable silt loams about 11in thick. Subsoil about 29in thick. Moderate permeability. Found on gently sloping land and on broad ridgetops. Well drained. Very micaceous. Water capacity is moderate to high and runoff is moderate. These are present southeast of the present study areas.

Mount Airy and Manor silt loam (MOC: 8-15% slope and MOD: 15-25% slope) - These soils are excessively drained deep silt loam (Mt. Airy) and very deep loam (Manor). They are found on broad ridgetops and side slopes. They tend to be dark brown and friable, with 8in of soil thickness and subsoils ranging from 12-16in thick. In some locations the depth to bedrock may be less than 60in. Both have medium permeability, with low water capacity, and medium to rapid surface runoff.

Conestoga silt loam (CnB: 3-8% slope) - These soils are gently sloping, very deep, and well drained, found on undulating, broad uplands. The soil is dark brown and friable, and is about 9in thick with a 31in thick subsoil. Permeability is moderate, water capacity is moderate to high, and runoff is medium. This is the primary soil unit that underlies the study area and which sits upon the Vintage Formation.

Lindside silt loam (Lw: 0-3% slope) - This soil occurs in areas that are nearly level (e.g. flood plains), are very deep, and are moderately well drained. The soil is friable, dark brown, and tends to be about 10in

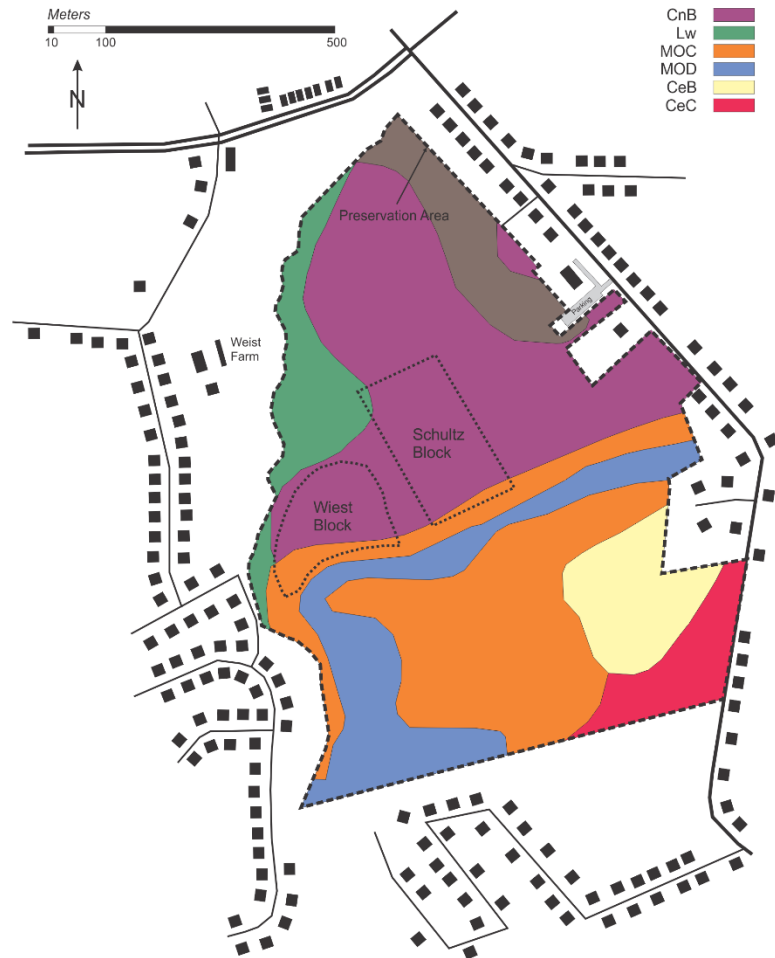


Figure 8. Soils within the Camp Security protected area.

thick with a 23in thick subsoil. Permeability is moderate at the surface, decreasing with increasing depth. Water capacity is high to very high and runoff is slow. The soil is subject to frequent flooding.

Within the study area the underlying quartzite, dolomite (limestone), shale, conglomerate geologic units produce silty loams soils. These soils tend to be relatively well drained, with depths of approximately 8 to 10 inches. The subsoil layer below this ranges from 20 to 40 inches in depth, but as indicated in geophysical investigations herein, could be somewhat thicker due to karst development. Given these conditions, the typical stockade trench that one would expect to find associated with a prisoner of war camp would likely penetrate into, but not through, the subsoil layer. Both ground penetrating radar and electromagnetic (EM) induction techniques work well in this type of environment, and should be able to detect any subsurface features associated with human activity.

METHODS

Given the current land use requirements of the field site (crop farming), the field work reported herein was completed primarily in the winter and early spring of 2017-18 (December to March) in order to stay off the site during the growing season. Initial site visit with Friends of Camp Security, senior archeologist Steve Warfel, and faculty researchers in the Department of Geography & Earth Science at Shippensburg University took place on December 11, 2017. The initial site visit informed our planning for the geophysical surveys and a plan was put in place to work around the construction footprint for the Springettsbury Township sanitary sewer being constructed on site (Figure 9).



Figure 9. Photograph taken on 12/11/2017 from the SW corner of the Wiest block showing the footprint of work on the sanitary sewer. View is to the north. Shultz farmhouse is visible in the background to the east of the constructed equipment/pipeline access road.

Initial field work commenced on 1/09/2018 with GPS mapping. The majority of GPR surveys were completed on 1/19/2018 (Wiest Block 10m grid), 3/10/2018 (Wiest Block 1m grid), 3/13/2018 (Schultz Block 10m grid), and 3/15/2018 (Schultz Block 10m grid and Wiest Block 1m grid 2). The EM surveys were completed on 3/10/18 , 3/13/18, and 3/15/18 (Wiest block) and 4/21/18 (Schultz block).



Figure 10. Photographs of volunteers beginning to open the hedgerow between the Schultz and Wiest blocks on 1/17/2018. Pruning shears, chainsaws, and heavy-duty loppers were required to open a clear line-of-site and an access trail between the two blocks. The photograph top right shows the line-of-site once it was opened up. In the foreground is the Trimble GPS sitting on a previously established benchmark (Benchmark 7).

Site Preparation

Numerous volunteers from the Friends of Camp Security and the senior archeologist are commended and graciously acknowledged for their support to complete this study. Their help was important to prepare the site (significant shrub removal to complete line-of-site vantage points to link the Wiest and Schultz blocks) for mapping and also to lay out the grids that were used to facilitate geophysical and topographic data collection (Figure 10). We also acknowledge the assistance of students from both Shippensburg University and Millersville University for their assistance with field logistics and data collection.

Topographic Mapping

Initial mapping commenced on 1/9/2018 when surveying sets used in previous archeological investigations were identified and mapped using a Trimble GeoExplorer CE GPS with an external antenna (Figure 11). Weather and snow conditions prevented use of geophysical instrumentation on this date, but we worked to identify previous landmarks and establish new benchmarks for topographic and geographic referencing. These benchmarks are identified in Figure 12. Additional Trimble GeoXT GPS units were used for mapping point, line, and polygon feature classes throughout the study. The coordinates for surveying set points or benchmarks and other landmarks are provided in the attached geodatabase. Horizontal accuracy with the Trimble



Figure 11. Photograph of GPS with external antenna used in this study.

GeoExplorer CE system was 30cm and the vertical accuracy is approximately a meter. All points in the geodatabase were referenced to NAD 1983 State Plane Pennsylvania South FIPS 3702.

Topographic profiles were collected on 3/3/2018 using two TopCon GTS220 Total Stations. Two teams were assembled to survey the Schultz and Wiest blocks respectively and standard survey reflectors and poles were utilized. In total 336 occupied position points (i.e. with northing, easting, and elevation coordinates) were collected from the Wiest Block and 125 points were collected from Schultz. Figure 13 is a scatterplot of all topographic points collected in the Wiest block from Benchmark 6.

Additional points on this grid show the positions of the stream banks and stream bottom in the line-of-site through the hedgerow, as well as the position of Benchmark 7 (in the NE corner of the grid or upper right side in the plot). As shown the total relief for the Wiest block was approximately 50 feet from the north to the south end of the transect sites. A notable change in slope is present in the southernmost part of the block. As noted previously, this change in slope is tied to a significant change in subsurface bedrock lithology from more resistant beds (the Antietam) to less resistant beds (the Vintage). Moreover, it is likely that fractures, joints, and changes in porosity/permeability in these units contribute to and help control the location of springs and stream morphology as noted earlier. All data points were imported into both the geodatabase as well as software for GPR analysis as discussed below.

Mapping Grid Layout

In order to prepare each site for geophysical investigation, surveying grids were installed on the landscape using orange and black plastic surveying pins. Once a corner pin position was located, large 100m surveying tapes were used to square off the grid end lines and subsequent pins were driven into the ground at 10m spacing (east-west) and at 20m spacing (north-south; Figure 14). A large steel digging

Benchmark/Location	Easting	Northing	Elevation
6 – North Wiest Block	2277790.9	235482.7	445.5 feet
7 – West Schultz Block	2277998.2	234949.6	487.2 feet
8 – South Wiest Block	2277999	234947	491.8 feet



Figure 12. Benchmark locations and coordinates.

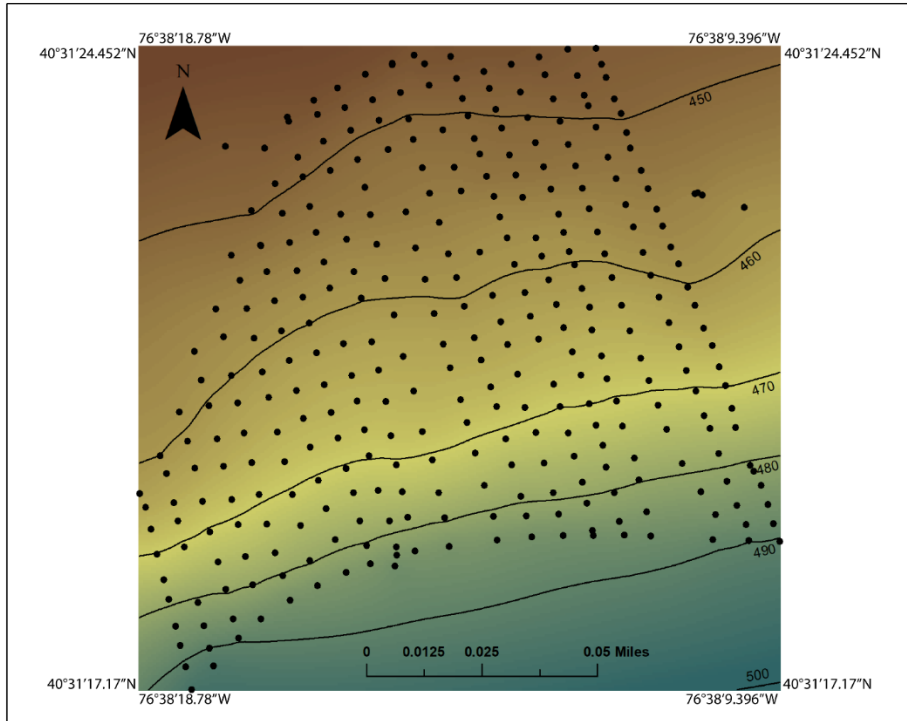


Figure 13. 3D Map showing N, E, Z grid points for Wiest block survey. Contour lines are in 10' increments

bar was required to break through the frost so that all pins could be driven into the ground. Once the initial grids were established, orange flagged surveying stakes were used to demarcate specific surveying transect lines to be investigated. Orange flags were also placed at the mid-points of transects to assist with navigation. Given guidance from previous archeological investigations, it was deemed important to begin in the Wiest block. Subsequent mapping grids were

installed on the Schultz block. In both blocks, initial grids were laid out to provide a coarse resolution for initial GPR investigation.



Figure 14. Volunteers assisting in set-up of the southern boundary of the Wiest block using 100m surveyor's tape (left). Surveying pins demarcate the northern boundary of the Wiest block (right). View is to the east in both cases.

In the Wiest block, the initial transect was laid out at 10m east-west spacing and ran 160m north-south, so that surveyed transects were aligned parallel to the slope. At this scale 31 GPR transects (WB_1_19_18_0001 to 0031) were collected in roughly NW-SE running transects. Not all were successful due to weather conditions and battery life of the computer (23 were reasonably successful and provided



Figure 15. Photograph facing south (uphill) on the Wiest block. Image shows the layout of the Wiest 80x40mx1m grid from the NE corner of the grid. Orange flags were used to mark the north and south end points of the grid, as well as the 40m center line on each transect. Note this grid lies entirely west of the plowed area where the latest archeological test trenches were dug. The second 1m grid was installed in the uphill area visible in this image.

data that are discussed in the GPR section of this report). As a note of reference, this initial grid crossed the plowed zone (i.e. the area of earlier archeological trench excavations) and extended to the west toward the excavations for the Springettsbury sanitary sewer project. This low resolution grid was



Figure 16. Photograph of the Schultz block looking northward toward the Schultz farm. Clearly visible in the mid ground of the image is the recent plow zone where archeological investigations were completed in 2016. Initial 10m transects were installed to run up/downhill.

supplemented with higher resolution 1m grids installed in areas where the initial GPR returns (once processed) indicated anomalous features in the target zone. Thus two additional grids were installed (Figure 15). One was a 80m x 40m grid to facilitate a 1m transect spacing for both GPR and EM studies

(i.e. for GPR profiles: WB_3_10_18_0001 to 0041), and the other was a 50m x 25m grid also at 1 m spacing (GPR Profiles: WB_3_15_18_0001 to 0024).

For the Schultz block, grids were laid out similarly with an initial large grid initiating at the southern tree line closest to the Wiest block and extending northward toward the farm house. The initial grid was 270m x 140m and transects were collected at 10m spacing (GPR profiles SB_3_13_0001 to 0016). Again as with the Wiest block, transects were oriented to run parallel to the slope as shown in Figure 16. Once anomalies were identified, two days later, a smaller 80m x 40m grid at 1 m transect spacing was installed (SB_3_15_0001 to 0041). In addition to these 5 primary grids, one additional smaller grid was completed for EM analysis in the Wiest block to follow a trend noted in preliminary EM results. This is described elsewhere in this report. All survey mapping grids are recorded in Table 1 with their accompanying GPR profile labels and surveyed transects are included in Figure 17.

Table 1. Profile name includes the date of data collection as the prefix to the incremental transect number.

Block & Grid Description	GPR Profiles
Wiest 1 (100m x 160m with 10m transect spacing)	WB_1_19_18_0001.rd3 to 0031.rd3
Wiest 2 (80m x 40m with 1m transect spacing)	WB_3_10_18_0001.rd3 to 0041.rd3
Wiest 3 (50 m x 25m with 1m transect spacing)	WB_3_15_18_0001.rd3 to 0024.rd3
Schultz 1 (270m x 140m with 10m transect spacing)	SB_3_13_0001.rd3 to 0016.rd3
Schultz 2 (80m x 40m with 1m transect spacing)	SB_3_15_0001.rd3 to 0041.rd3



Figure 17. Overview map that shows all grids for the survey. 10m grids shown as lines, 1m grids shown as polygons.

Ground Penetrating Radar (GPR)

Although not ideal for shallow geophysical surveys, data collection took place when the ground was still frozen and primarily snow-free. As noted previously, weather conditions presented a number of challenges for this investigation. First, field work did not occur during late January and February due to accumulating snow events, and below zero temperatures. Severe cold limits equipment functionality including battery life, and excessive snow/ice accumulates on the GPR signal trigger wheel and prevents it from turning and triggering effectively. Moreover, GPR survey responses, in particular, can be influenced by soil and surface conditions. It was therefore important to attempt data collection under similar conditions throughout the duration of data collection and to limit field work to snow/ice free days if possible. However, thin accumulations of snow/ice were present on two days of data collection (January 19, 2018 and March 10, 2018). On both occasions the snow melted during the course of field work and radar returns produced usable GPR data and were not appreciably different because the ground was still frozen in each case.

As shown in Table 1, GPR transect data were collected on 4 different sampling dates, primarily in mid-March. GPR or Ground Penetrating Radar can be a very useful geophysical method in non-invasive shallow subsurface investigations depending on the composition of subsurface materials. As a method, it relies upon the ability of high-frequency sound (radar) waves transmitted into the subsurface (at velocities of roughly 3.00×10^8 m/s) to reflect off subsurface discontinuities without absorption. Under ideal conditions the majority of radar waves will bounce back to the receiver on the instrument and a two-way travel time (time down and back) can be measured (Figure 18). Given a known or assumed travel velocity (note that different subsurface materials will have different velocities) a simple algorithm in the data acquisition software will measure signal response and calculate approximate depths. The software then converts these data into a 2D visualization that integrates measurements from stacks (repeat samples) of transmitted/received signals for each horizontal position in order to identify subsurface anomalies. Each transect thus produces a vertical profile or trace from the ground surface down to a set depth called the *time window*. In this study the time window was set to be 100 nanoseconds (~ 15 feet below the surface) for this survey. This is well below the area of interest for most archeological investigations which are typically less than 2 meters for most features.

Signal reflections or subsurface anomalies are produced in GPR returns due to changes in dielectric properties of subsurface materials. Subsurface materials will have a wide range of dielectric properties and therefore will either be prone to attenuation (absorption of sound without reflection) or will be prone to reflection. For instance, air has a very low dielectric constant of 1 and an attenuation of 0 decibels/meter. This means that radar will not generally attenuate in air until it strikes a material that is absorptive or it strikes a material that is reflective (high dielectric constants). When the radar initially leaves the transmitter the first discontinuity it experiences is the ground surface and this typically reflects a significant portion of radar. However some radar is transmitted down into the subsurface where it can interact with other materials including groundwater, soil horizons, rock horizons, or anthropogenic features that have distinctive dielectric permittivity. The best signal reflections occur when the dielectric properties are distinct and sharp. Gradational contacts or broad contacts are typically difficult to resolve.

For instance, in the subsurface fresh groundwater and saturated sands have high dielectric properties and generally low attenuation and are therefore favorable for GPR studies especially when they are interbedded with contrasting lithologies. Some materials including saltwater, peats, or pure clays (which have high conductivities), in contrast, all tend to have high attenuation despite their dielectric properties. Thus subsurface intervals dominated by these materials tend to be unfavorable to GPR investigations. The frozen silty loam soils that are found at the Camp Security site have dielectric

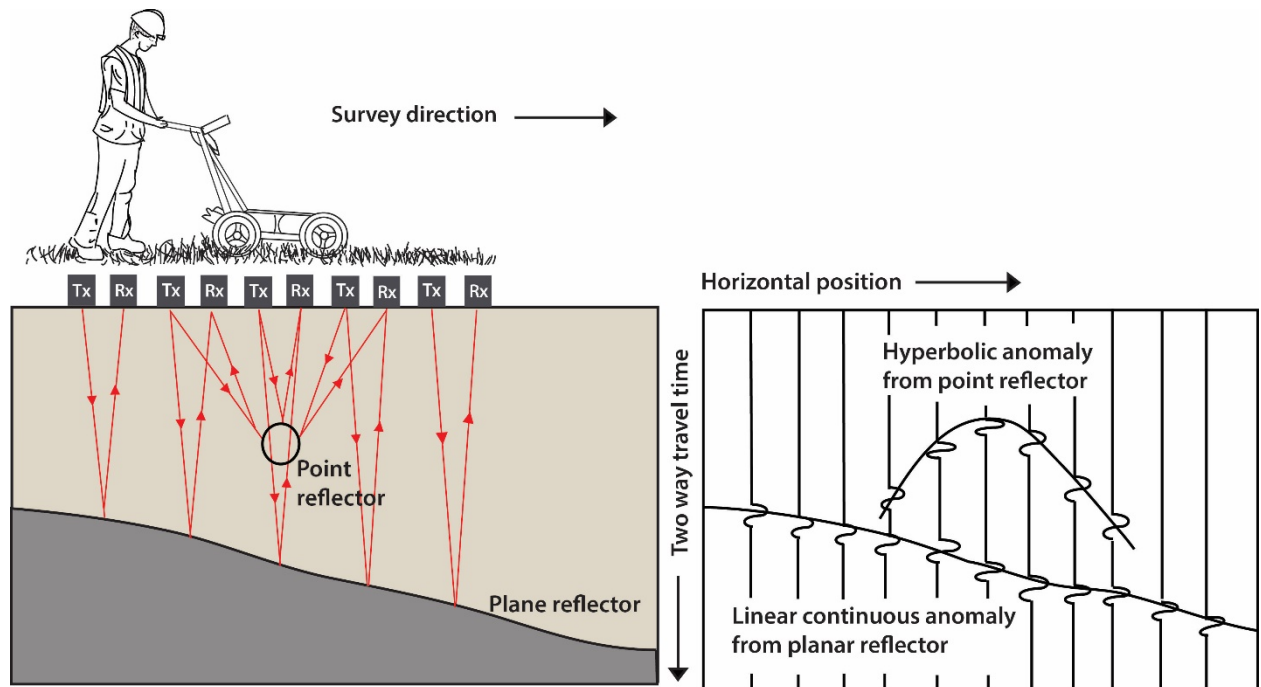


Figure 18. Graphic demonstrating basic equipment set-up and data acquisition theory. As shown in the left side, the transmitter (Tx) sends stacks of radar signals at each horizontal trigger position along the survey line. Depending upon the nature of the subsurface discontinuities (in this case a planar and a point feature are diagramed) different responses will be generated in the visualization as radar returns to the receiver (Rx). Each individual pulse produces a trace response and is output through the software. Planar features (i.e. bedrock contacts, distinctive bedding in soils, water table, etc.) are recognized in the 2D signal response (image above right) once multiple traces are juxtaposed next to each other in the visualization. Point features (i.e. void spaces, pipes, float stones, etc.) are typically identified by hyperbolic reflectors centered on the position of the point feature. These hyperbolic reflectors are the result of changes in distance from the Tx/Rx as the GPR is moved along the transect.

constant values that are assumed to be variable, but moderate (5 to 30) in contrast to that of freshwater or saltwater or clay soils. Silty soils tend to have higher attenuation values that approach 100 decibels/meter (so very little signal is returned from deeper features). This can limit the signal response and reduce radar returns. However when frozen these attenuation values have been shown to decrease as ice (water frozen in clay/silt-rich soils) can expand and sound can travel more readily. Since our area of interest is very shallow, the conditions for GPR have been improved demonstrably. So although silty soils with high organic components can in some cases be problematic for GPR investigations, when frozen they are less problematic for investigations of this type. Thus, although the conditions at Camp Security site are not perfect conditions for GPR investigations, the results of this study show that it is possible to collect reasonable datasets.

Table 2: Ground Vision parameterization

Sampling Frequency	5022 Mhz	Time Window (ns)	101
Number of Samples/Trace	506	Trace Interval (m)	0.05
Number of stacks	8	Antenna Separation (m)	0.180 (fixed in 500 Mhz)

For this study, we utilized a Mala Geosciences X3M GPR control system, with a 500 Mhz shielded antenna with a trigger wheel as shown in Figure 19. RAMAC GroundVision software loaded onto a ruggedized field laptop was used. The parameters for the control unit were set within the software to program and record all data from each transect. Table 2 shows the parameters used in this study. Figure 20 shows a representative radargram as viewed in GroundVision. Once initial 10m transects on



Figure 19. GPR set-up showing 500 Mhz antenna with triggering wheel attached.

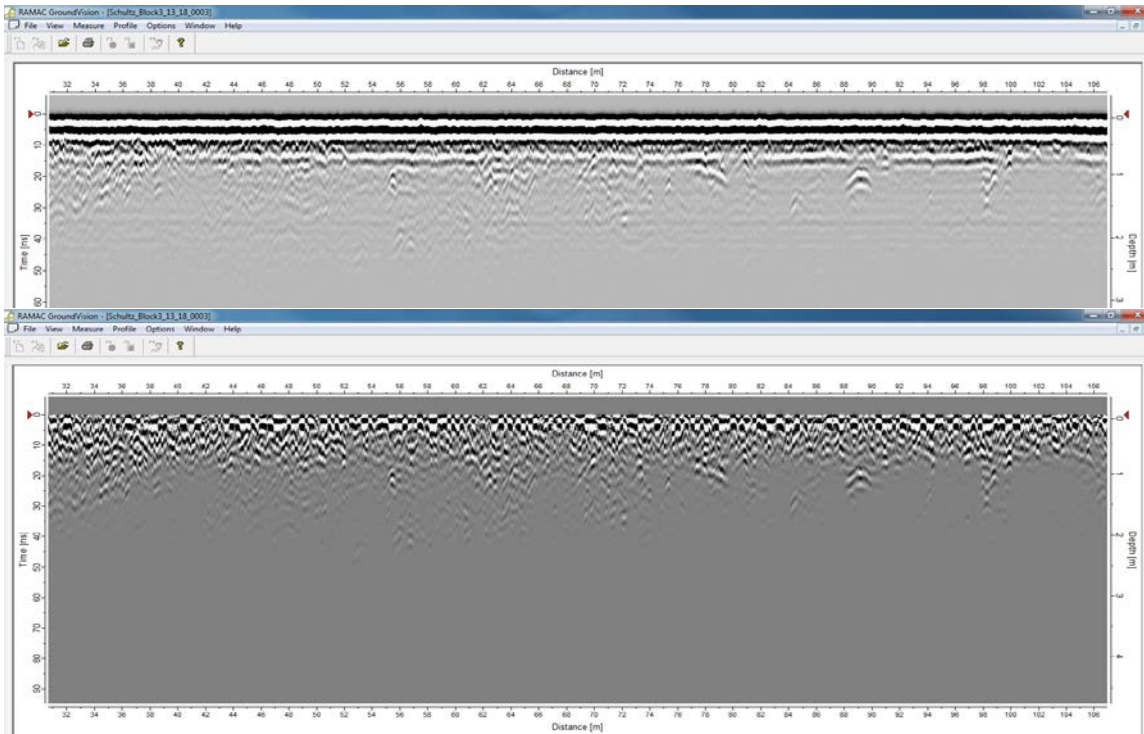


Figure 20. Radargrams from Schultz Block for the exact same interval. Raw unprocessed radargram (top), bottom is the same radargram with two filters applied (DC Removal and Background Removal) used to help remove the ground surface radar response overprint while enhancing the more subtle anomalies.

the Wiest and Schultz block were sampled each radargram was reviewed to a limited extent during data collection, but primarily after field work was completed in order to investigate the presence of anomalies within the target zone. These were then used to refine a search area for high-resolution investigation. For this study the target zone was below the plowed zone (topsoil) which extended down to about approximately 15", but above bedrock (Figure 21). Most anthropogenic features would be present in the subsoil down to no more than 1.5 to 2m, except in the case of a buried well which might be deeper. So ideally features located in the 0.25 m to 1.5 m interval would be candidates for investigation. As shown in the screenshot of the radargram from Schultz Block in Figure 20, the top,

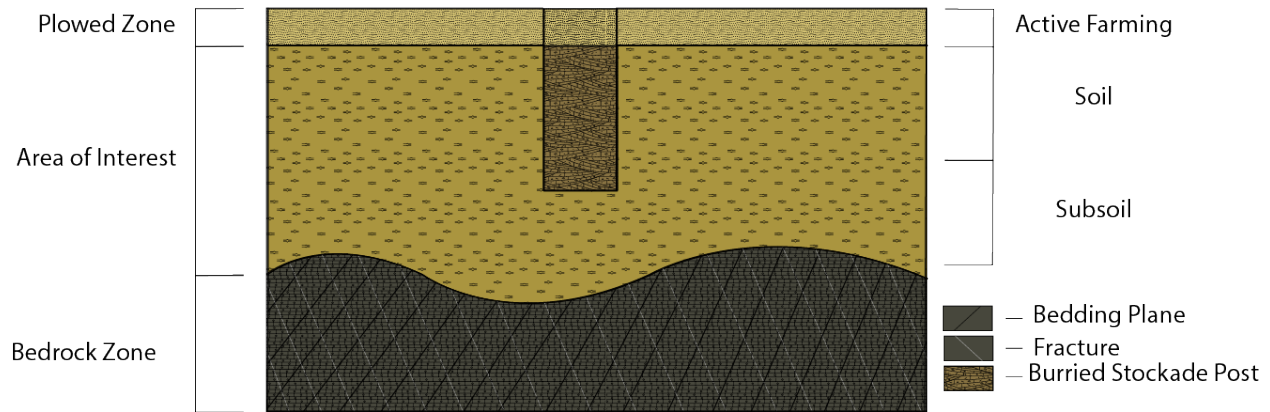


Figure 21. Hypothetical cross-section of subsurface intervals investigated with GPR in this study. The target interval or area of interest lies immediately below the tilled horizon in the topsoil and above the bedrock contact. It is this interval where trenches for stockade posts would be most readily located. Dielectric differentials should be pronounced between the subsoil and bedrock, although highly weathered shale and limestone bedrock with extensive C horizon will likely make this contact more obscure and diffuse. Moreover clay-rich intervals and shale (or other high conductivity materials) will attenuate radar, and will result in decreased depth of investigation.

unfiltered radargram shows a prominent linear anomaly (black-white-black-white band) located at the top of the radargram. This is clearly the ground surface and the uppermost topsoil interval and is the primary radar response and this can often swamp the radar signals from deeper targets.

Additional yet more subtle features are identifiable below the ground surface and these features occur within the target depth interval. In order to enhance these more subtle features, data acquisition software and post-processing software can be used to apply filters to remove the overprint of strong signals in order to enhance the weaker signals from other subsurface features. Figure 22 provides an overview of the basic data processing work flow used in this study. Once data is acquired in the field, basic analysis of the raw data was completed in the field, but with limited capacity for interpretation. Once data files are closed and written, more substantive post-collection data processing can take place to further improve the fidelity of the data so that it can more readily be interpreted.

For instance, the image at the bottom of Figure 20 shows the same region of the radargram with two filters applied. Once applied, these reduce the strength of the surface return, thus subsurface features down to about 2 meters are more readily discernable. In this case, few linear anomalies are identifiable in the portion of the radargram shown. However numerous hyperbolic point reflectors at a range of depths are indicated. In this image one key feature is located at 89 meters along the transect and at a depth of 80-90 cm. Another is located at about 55.5 meters at a similar depth.

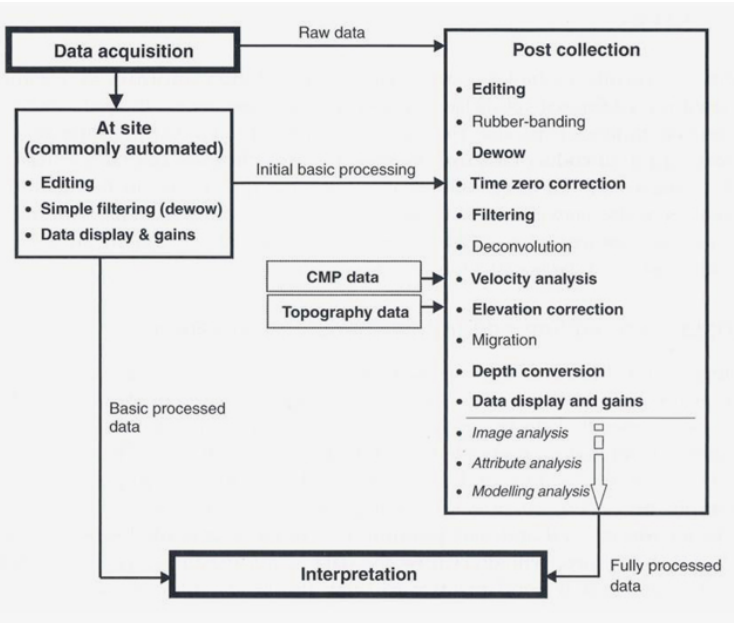


Figure 22. Overview of the basic data processing work flow used in this study.

obvious anomaly. For each position along the transect, the depth to no return is variable. The signature of the “no return” is the depth below which (after background removal) little radar energy is reflected back to the surface. This is evidenced by the loss of the black-white-black patterning and replacement by the medium gray solid color. Although more detailed post-collection processing can be utilized to help improve and amplify the returns, the time and effort for the purposes of this study are not necessary. That said a quick post-processing routine was completed within the GPRSlice software (see below) to visualize these radargrams in color format before and after filtering using only background removal. Figure 23 shows the second transect on the Shultz Block and this radargram is oriented from south (uphill) to north (downhill). Top and bottom images in this figure show the differences between raw and filtered data (background removed). The major disparity recognized here is in the thickness of the subsoil interval. On southern end (uphill) bedrock is clearly present nearer the surface. Progressing northward, the depth to bedrock increases dramatically at 110 m and soil/subsoil is thicker to the end of the profile, although the bedrock subsoil contact appears to shallow and deepen across the profile likely due to pinnacles in the bedrock. Given this scale of observation, several small, shallow hyperbolic anomalies are noted above the inferred bedrock contact and these reflectors are concentrated in the 150m to 180 m range (at depths down to ~1 meter). Another set appear in the 45 to 80 m range. One of these hyperbolic reflectors aligns with the water pipe to the farm house.

As illustrated here, using the 2D vertical slice radargrams alone is inconclusive for identification of specific features. Additional methods can be applied to not only enhance individual radargrams (i.e. through the use of RadExplorer Software) to improve their interpretation, and correct for topography, but also to produce 3D map view visualizations. As such, the additional method employed here uses GPRSlice which is a software that allows the post-processing of radargrams to produce a 3D matrix to further assess trends in anomalies. GPRSlice software works to integrate multiple 2D radargrams into a coordinate grid. When 2D transect radargrams are collected at closely spaced (i.e. 1m) intervals, the software is used to interpolate between neighboring lines in 3D space. This allows the user to not only visualize the radargrams in plan-view, but it also allows for the creation of map-view slices from the surface downward across the gridded area. Moreover, this software allows the user to select different

Although similar in hyperbolic pattern these features have different shapes indicating differently sized/shaped features, but are disconnected from the surface and overlain by materials with different dielectric properties. Another hyperbolic anomaly is identifiable in this radargram at 100 meters. This feature is less symmetrical, a bit shallower and more importantly clustered with other anomalies.

The radargrams in Figure 20 (produced in GroundVision) show an even more subtle and certainly less

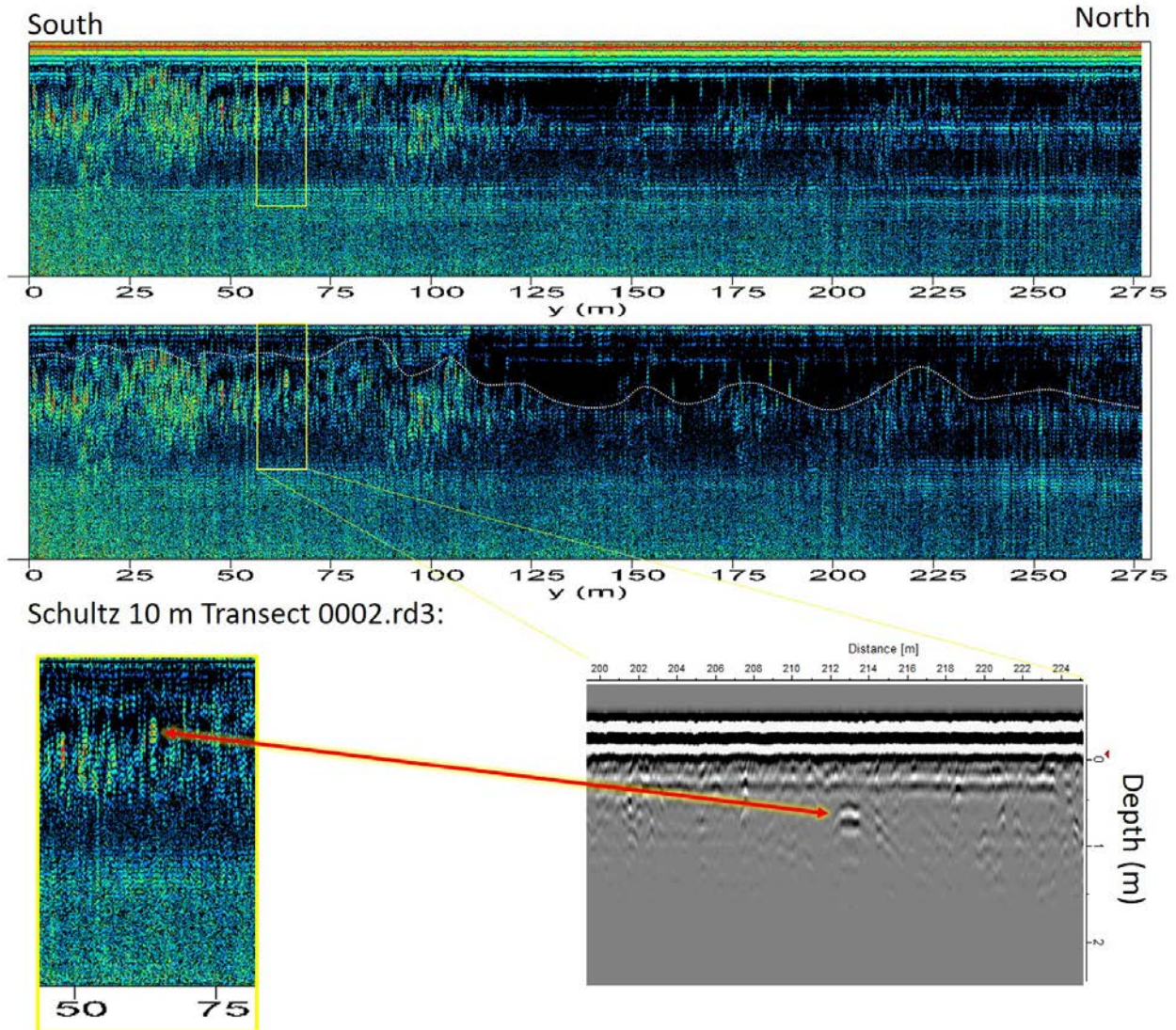


Figure 23. Top: Raw radargram collected with 500 MHz X3M; Middle: Same interval processed with background removal to remove time zero surface noise. Dotted line in the lower radargram is the inferred position of the subsoil-bedrock contact. Depth range for the entire window is to 100 nanoseconds (~4.5 meters based on 10cm/ns ground velocity). Bottom: Water pipe anomaly noted on radargrams.

color ramps to represent the data so that different features might be more readily identified (relative to traditional grayscale outputs) as shown in other radargrams (Figure 24). In this study, GPR slice was used only with the high-resolution (closely spaced) datasets. It could not effectively be used to evaluate the low-resolution (10m spaced) grids. In order to best interpret the data collected, significant effort was made to map the location of features created by previous archeological investigations and to locate existing depressions, groundhog holes, plowed areas, tractor/truck ruts, pipeline construction materials, etc. Where visible in the land surface, these were mapped using the GPS unit as noted and integrated into the geodatabase that serves as the primary GIS system for this and future investigations. Although most of these are evident only at or very near the surface, some have sub-surface expressions, so this database was referenced in order to eliminate known features.

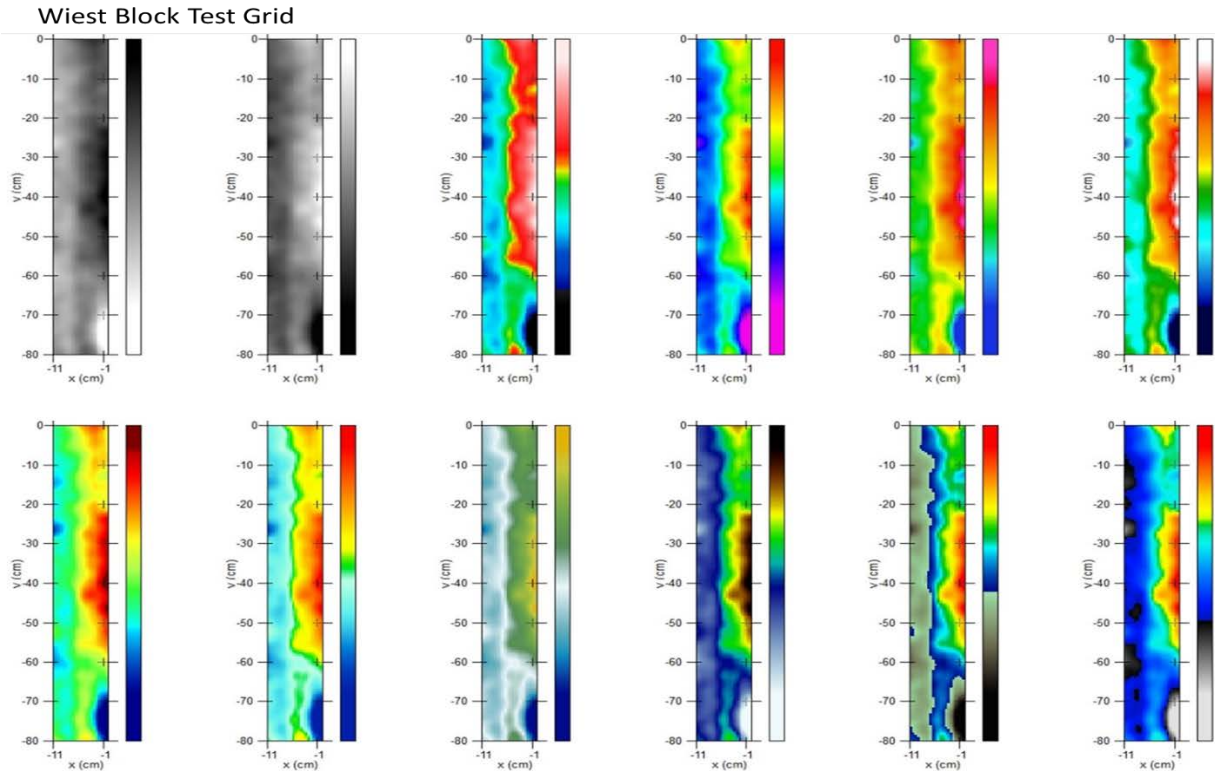


Figure 24. Colorized map-view output options for a test run of the Wiest block data. All outputs are colorized for the same depth slice using different color ramp options across a 12m x 80m x 1m grid spacing. As shown black and white outputs limit the visualization and interpretation of extremely positive responses from extremely negative response values. In general for most of these color ramps, positive dielectric shifts are represented by warmer colors whereas negative are cooler.

Electromagnetic (EM) Induction

The electromagnetic (EM) induction method is an electrical geophysical technique that maps subsurface conductivity. Under ideal set of conditions, EM surveys can detect archaeological features such as refuse dump sites, building foundations, ditches, graves, among others, on the basis of contrasting conductivity signatures. However, under extremely wet soil conditions, the abundance of soil moisture raises the background conductivity of the near surface zone, making it difficult to delineate anomalous areas with certainty.

The working principle of the EM method is straightforward; current is passed through a transmitter coil (Tx), which creates a primary electromagnetic field in the coil. The primary EM field travels underground and induces electrical currents in subsurface materials. The induced currents, in turn, generate secondary electromagnetic fields that travel out to the surface and are picked up by a receiver coil (Rx). The strength of a secondary field generated is directly proportional to the apparent conductivity of the material producing it. Thus, the EM method distinguishes subsurface features on the basis of their electrical conductivities. Figure 25 shows the EMP Profiler, the equipment used for this survey. The profiler is a frequency domain EM unit manufactured by GSSI Inc. It operates on a range of frequencies from 1kHz – 16 kHz and has a vertical resolution of up to 1.5 m. For the features of interest at Camp Security, this resolution was adequate.



Figure 25. Data collection using the GSSI EMP Profiler unit.

The EM data collection effort was aided by insights from preliminary GPR interpretation. Thus, EM grids were laid out over areas that GPR radargrams indicated high reflectivities of the transmitted radar pulses. All EM data were collected on rectangular grids with transects separated from each other by 1m. EM data could be collected on 3 frequencies simultaneously; however, the 15kHz Hz frequency must be chosen for accurate results because the algorithm for converting the quadrature values to apparent conductivity has been optimized for the 15 kHz frequency for the unit's coil spacing. All data were collected in the continuous mode (data recorded every second) with the vertical dipole mode coil orientation (antenna coil parallel to the ground surface). Data collection on the Wiest block commenced on 03/10/2018, on a 40 x 80m grid. However, the first effort did not go smoothly as data collected on the first half (20 x 80m) of the grid were lost due to battery failure. Nonetheless, those collected on the second half were successfully saved,

downloaded, and processed (named Grid 016). On this grid the EMP's internal GPS was set to collect data location coordinates. Additionally, a Trimble GPS unit was also used to collect coordinates at the four corners of the grid (See Figure 16 above).

Additional EM data were collected on the same corner of the Wiest block, on 03/13/18 and 03/15/18 respectively. On the 13th, data were collected from a 16 x 60 m grid (named Grid 021), offset to west of the previous 40x80 grid. On the second day, the EMP unit had lost its internal GPS communication, hence, coordinates of the grid corners were taken with a Trimble GPS unit. Another 12 x 40m grid (named Grid 022) was established to the west of Grid 021 and data collected. The final EM data collected from the Wiest block occurred on 03/15/18. A 22 x 50m grid (named Grid 027) was offset to the west and south of the previous grid. High conductivity readings were observed at the southern end of Grid 027. To get a more complete picture of this anomaly the southern 22 x 20m section of Grid 027 was reexamined but the traverses were along the X- rather than the Y- (E-W) directions. This grid named Grid 028.

Similar to the Wiest, the EM survey on the Schultz block was concentrated in a section where GPR anomalies were detected. The survey was conducted on 04/21/2018, on the same 40 x 80m grid used for GPR data collection and named Grid 031.

DATA RESULTS & INTERPRETATION

GPR Results

Over the course of 4 days of GPR data collection, a total of just over 8 km of low-resolution (10m grid spacing) radargrams and an additional 7.5 km of high-resolution (1m grid spacing) GPR radargrams

were collected. Thus in total, over 15.5 km of 2D GPR data were collected over the Wiest and Schultz blocks. Figure 26 shows the grid lines for the 3 high-resolution grids collected. As noted, all radar was reviewed in GroundVision and RadExplorer software for 2D investigation and imported into GPRslice for 3D time slice analysis. Raw radargrams for all transects are included in the appendices to this report. The task of reviewing all of 15.5 km of radar returns is a significant one and will require further time to more carefully and thoroughly review each. As shown in Appendix 1, a very large number of features (over 125 individual anomalies) in 4 different categories have been tentatively identified just for the Schultz 80m x 40m x 1m block.

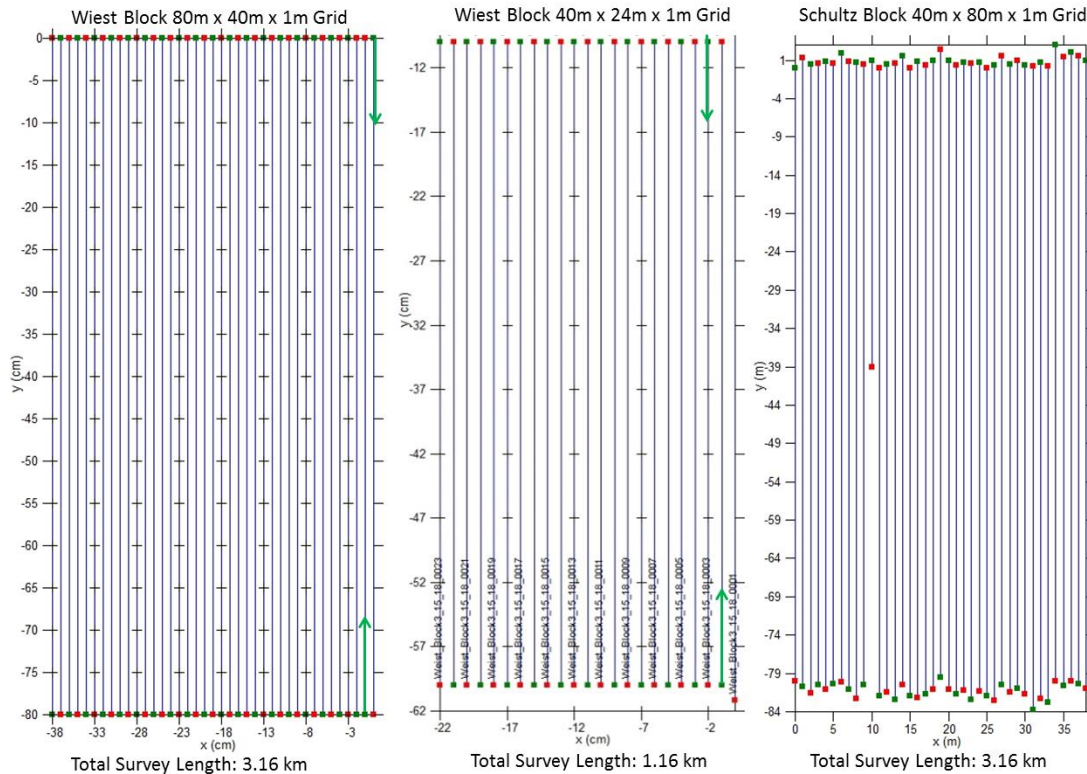


Figure 26. GPR transect lines for the 3 high resolution survey grids. Green block are start points, red are end points. NE corner of each is in the upper right. GPR started in the NE corner for the Wiest blocks and numbered sequentially westward, transects for the Schultz block in the NW corner and numbered sequentially eastward.

The four primary categories recognized include: Solitary (individual hyperbolas that are not co-located with other features), Grouped (hyperbolas that appear in clusters), Near Surface (hyperbolic features located near the surface and just below the topsoil), and Depressions (recognized as dipping reflectors that represent depressions in the planar tabular soil reflectors). Trenches, pits, sink holes, or similar features will result in depressions whereas float stones, pipes, void spaces, burrows, or foundation stones, or potentially stockade posts could produce point reflectors that present in radargrams as hyperbolic features. The established classification system of identified features was applied to each individual GPR transect to acquire a running tally of the total number within each category. Grouped hyperbolic point reflectors and planar reflectors oriented into depressions are most similar to features identified in the literature (See Appendix 2) and are therefore potentially important targets to investigate in the target zone of interest. Solitary hyperbolas may still be significant features; however, they could easily be a lone float rock, water pipe, or other geologic material with a highly resistive dielectric field surrounded by a material with weaker dielectric properties. Near surface

features are located above the target range and are more than likely associated to recent farming on the surface.

Given the other two high-resolution blocks, well-over 200 discrete features are recognizable, but most are likely natural features of little archeological interest. Significantly more data analysis time is required to run additional filters to enhance and evaluate other specific anomalies of interest. It is, however, a task that could potentially produce a very large and daunting number of anomalies that would be difficult to prioritize for further investigation. We therefore elected to pursue a different plan of action using the GPRSlice software to integrate 2D radargrams into 3D for a more integrated analysis approach (see below).

As shown previously in schematic Figure 21, the target interval for this study lies above the bedrock and below the uppermost top soil zone. Figure 27 below is a RadExplorer radargram (raw and interpreted) for the far western transect in the Wiest block. Careful examination of the radar returns enables the recognition of what is interpreted to be steeply-dipping, fractured and highly weathered bedrock at depth. Bedrock is present at depths ranging from less than 1m in the central and southern (uphill) parts of the transect. It appears that the bedrock is overlain by relatively horizontally-bedded soil horizons (planar-tabular reflectors) of variable thicknesses. Overall the soils are thickest in the northern portion of the transect. Soils appear to thin over pinnacles in the bedrock and thicken in troughs between more resistant bedrock pinnacles. Disruptions in these relatively tabular reflectors (i.e. below the upper topsoil) represent either natural subsidence or erosion processes or potentially anthropogenic disturbance. When studied at this scale, only large-scale features are readily observed. Smaller-scale features are harder to identify at this scale.

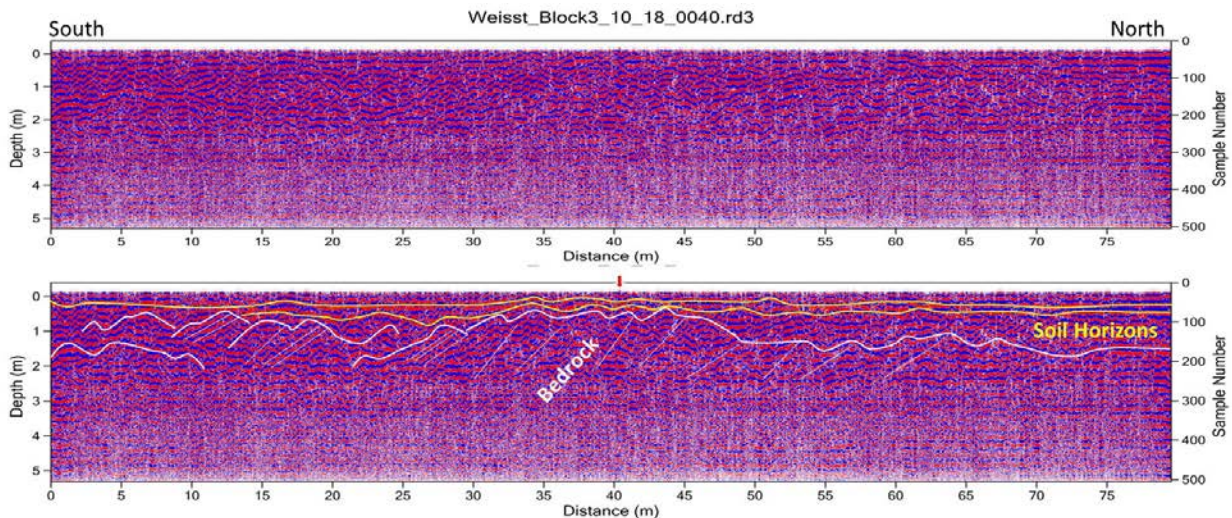


Figure 27. Radargram export from RadExplorer after filters were applied to remove the overprint of the surface time zero reflection and background radar response. Uninterpreted (top) and interpreted transect (bottom) for Transect 0040.rd3 located on the far western edge of the Wiest 80m x 40m x 1m grid.

In an effort to reduce the transect by transect review, our analysis time focused on importing 2D sections into the GPRSlice software. This enabled detection of more readily observable patterns between successive 2D transects. Figure 28 shows an output of our GPRSlice analysis for the Schutz block 80m x 40m x 1m grid. The diagram shows map-view time slices that range from the surface downward to an overall depth of about 2.4 meters which should be down below the subsoil and into the bedrock. Time slices for this output utilize all radar responses in cubic grid blocks of 0.25m x 0.25m x 0.3 m that are then integrated and averaged using an inverse neighbor weighting method set to calculate

across 1.5m cell blocks. The resulting output is then colorized to visually represent the numerical responses at each given time slice (depth interval) across the entire grid area. Data shown in this figure range from high positive radar response (red/orange) to a low negative radar response (deep blue). It is important to point out several artifacts of sampling procedure that are not factored out of the data. The metal surveying flags that were used to delineate end and midpoints of the grids produced a “ringing” in the data that are clearly observable at the very end of the transects as well as in the center at the 40m mark.

Irrespective of these artifacts, it is possible to observe several noticeable anomalies that are of interest. The surface slice (slice 1) is dominantly red and this represents the frozen topsoil zone that is highly conductive and has a high dielectric permittivity and a relatively low absorbance. Slice 2 is located below the frost line and an interesting 20m+ E-W oriented feature (strongly negative radar response) is identifiable. This feature appears to be about 2-3 meters wide in this analysis. It is also identifiable when the raw radargrams are processed through a background filter and a normalization function. Thus this feature has distinctly different dielectric properties from that of the surrounding materials. Other anomalies of interest (aka AOI’s) are summarized in Table 3.

In similar fashion to the high-resolution grid from the Schultz block, Figures 29 and 30 show additional time slice assessments for the two Wiest blocks. Anomalies of interest have been identified and are also reported in Table 3. Figure 31 was drafted to further investigate one of the more obvious anomalies in the Wiest 80m x 40m grid. This feature is identifiable as a highly positive radar response located in the SW corner of the NE quadrant of the grid. This particular feature is identifiable at the surface (even in recent aerial imagery from Google Earth (2016). As observed in the 2D cross-

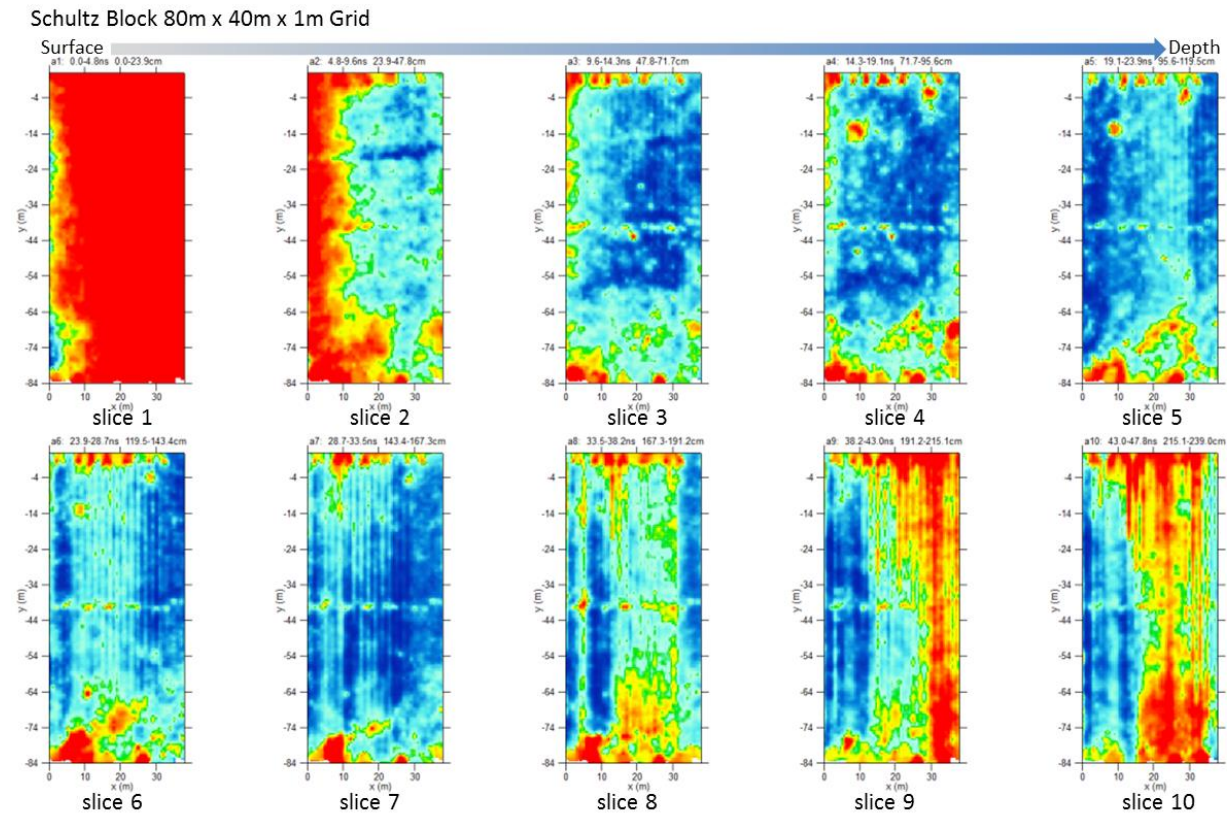


Figure 28: GPRSlice map-view time slices from the surface (slice 0) downward (down to slice 10) for the Schultz block (3_15_18 Data Collection). Each time slice represents approximately 24cm. No overlap in these time slices. Total depth represented by slices 1 to 10 is ~240 cm or 2.4 m.

sections of the feature shown in the GPR Slice map, the shallow soil planar reflectors (see the enlarged 2D radargram cross-sectional view at bottom center) indicate a 2.5m x 2.5m depression that extends from the surface downward to a depth of over 1.5 m and perhaps more. A second depression is also noted about 10m further north. This feature is more subtle, but is identifiable in the cross-sections of transect 0008, 0010 and 0012, but it definitely does not appear to be as deeply rooted. Based on this analysis, the more prominent feature is interpreted to represent either an infilled subsidence feature (sink hole) or an excavated circular pit that has been infilled.

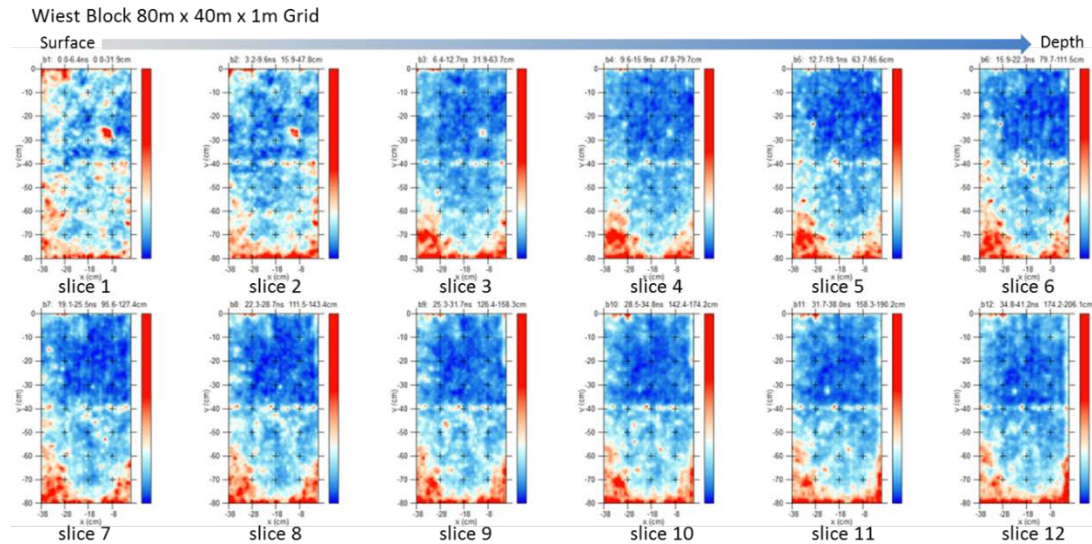


Figure 29. GPRSlice time slices from the surface (slice 0) to slice 12 for the Wiest block (3_13_18 Data Collection). Each represents ≈ 30 cm and overlaps above/below slice by 50%. Total depth ≈ 200 cm

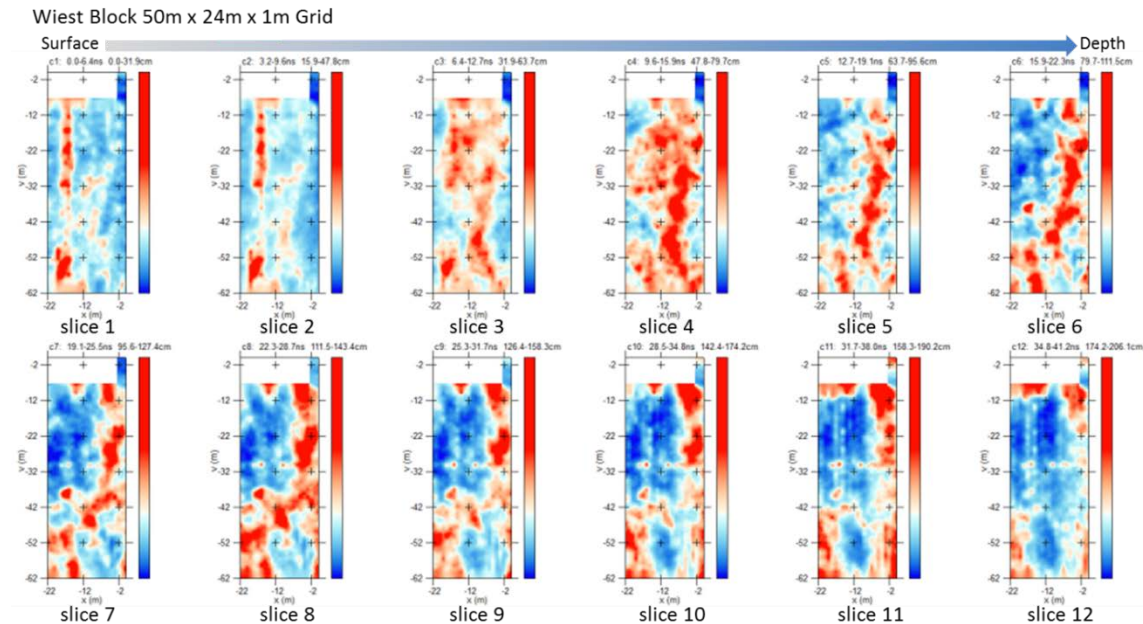


Figure 30. Similar GPRSlice time slices from the surface (slice 0) down to slice 12 for the Wiest block (3_15_18 Data Collection).

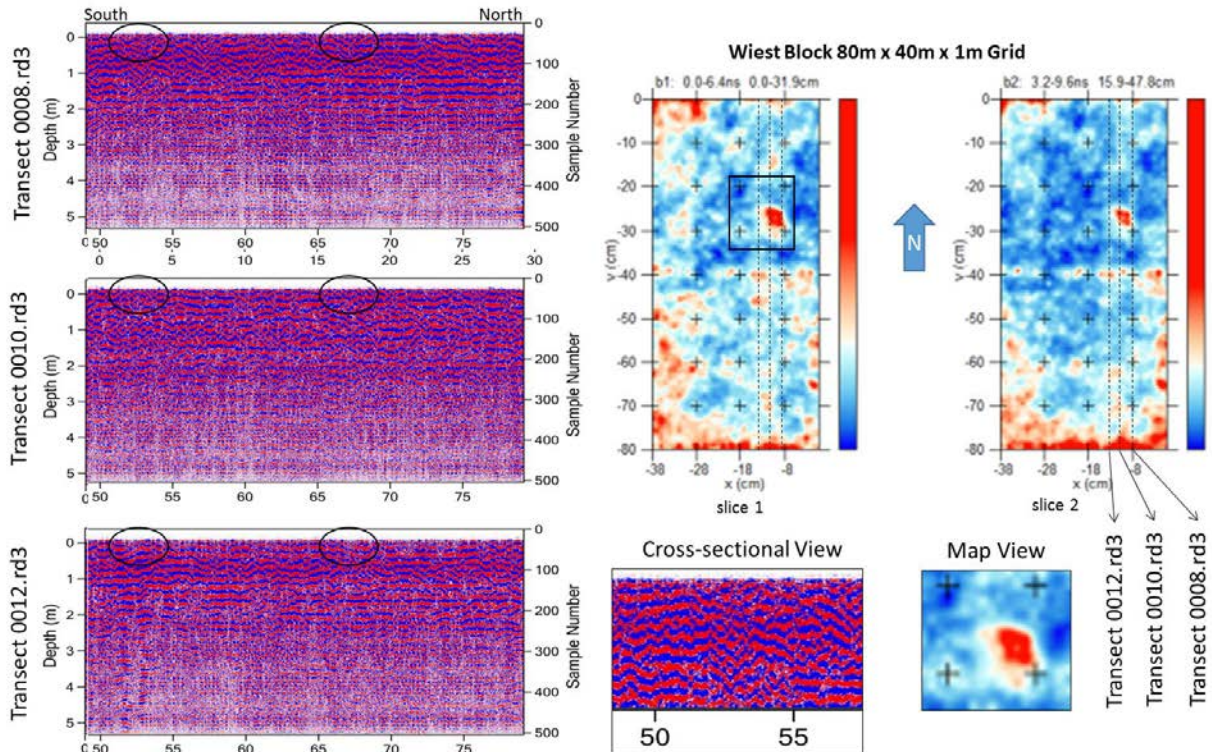


Figure 31. (Left) Anomaly of Interest (AOI) from Wiest block (WB1-1) shown from 2D vertical cross-sections from transects 0008, 0010, and 0012 which intersect the feature shown in the Map View time slice (upper right). Shown are time slices 1 and 2 which extend from the surface down to ~48 cm below the surface.

EM Results

Results of the EM data for the Wiest block analyses are presented in Figure 32. Conductivities on all grids within the Wiest block range from a minimum of 6 mS/m to a maximum of 13.5 mS/m, with the background conductivities in the range of 7-10 mS/m. Values above that range, enclosed by bold contours, are considered anomalous. Changes in soil moisture over the data gathering period have clearly altered the near-surface conductivity, and can be seen in the discontinuous conductivity readings between adjacent grids. However, a few patterns do emerge from these data. The large increase in conductivity seen in southern half of Grid 027 is the influence that the construction equipment had on soil compaction on the western side of the Wiest block. The size and shape of the anomaly is likely due to the combined influences of soil compaction and the spread of mulch across the area to prevent erosion. The large areas of high conductivity seen in the central parts of grids 016 and 021 are likely due to increased soils moisture from both snow melt and near surface water movement downslope. During our field work we noticed that the ground was often saturated just north of the break in the slope. The anomalies of most interest based on the EM data are the linear features seen in grids 021 and 022. The linear feature in Grid 021 displays a higher change in conductivity, but appears as discontinuous (marked in red). The linear feature in Grid 022, while not as strong, is more continuous. While both of these anomalies are intriguing, we must caution that they also run parallel to the subsurface geology and slope, and may simply represent saturated fractures in the rock or buried erosion gullies.

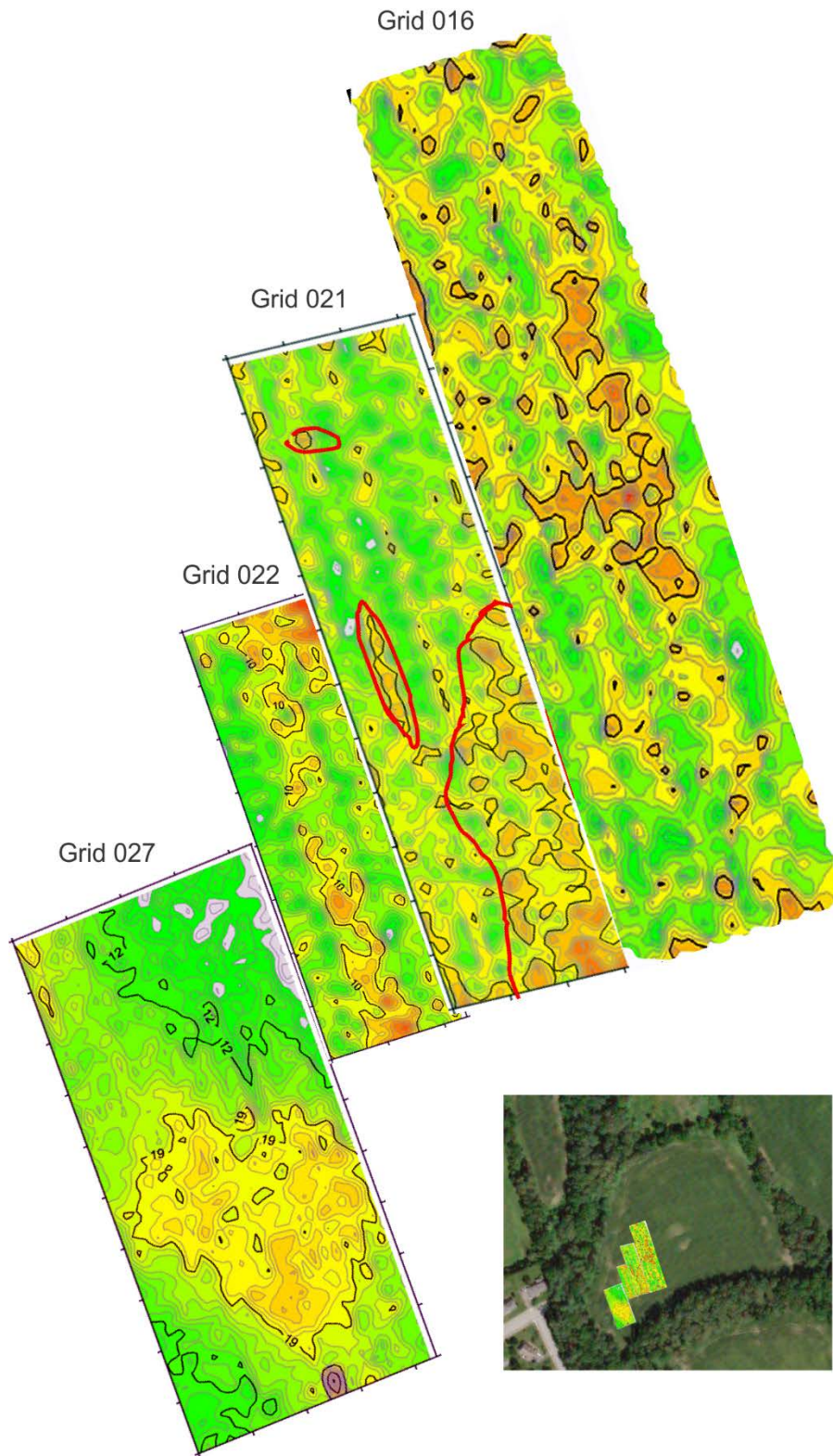


Figure 32. EM conductivity results from the Wiest block grids.

The EM result obtained on the 40 x 80 m grid at the Shultz location, is presented as conductivity contours in Figure 33. It should be noted that this survey was conducted when the grounds were fairly wet, hence the generally higher background conductivity values relative to the Wiest block. A wide conductivity range (7 – 36 mS/m) was observed. Areas standing above the background are enclosed by bold contours. However, the highest conductivities are observed as linear N-S bands on the left edge of the grid, with the first 13 m from the origin in the x-direction. It is not likely that these trends represent any obvious archaeological features in the manner depicted, and may represent a moisture gradient or near surface geologic structures. There were some elevated conductivity reading (> 16 mS/s) in the southwestern section of the grid that roughly correspond to the anomalies found in the GPR data; however, they appear indistinct in the EM data.

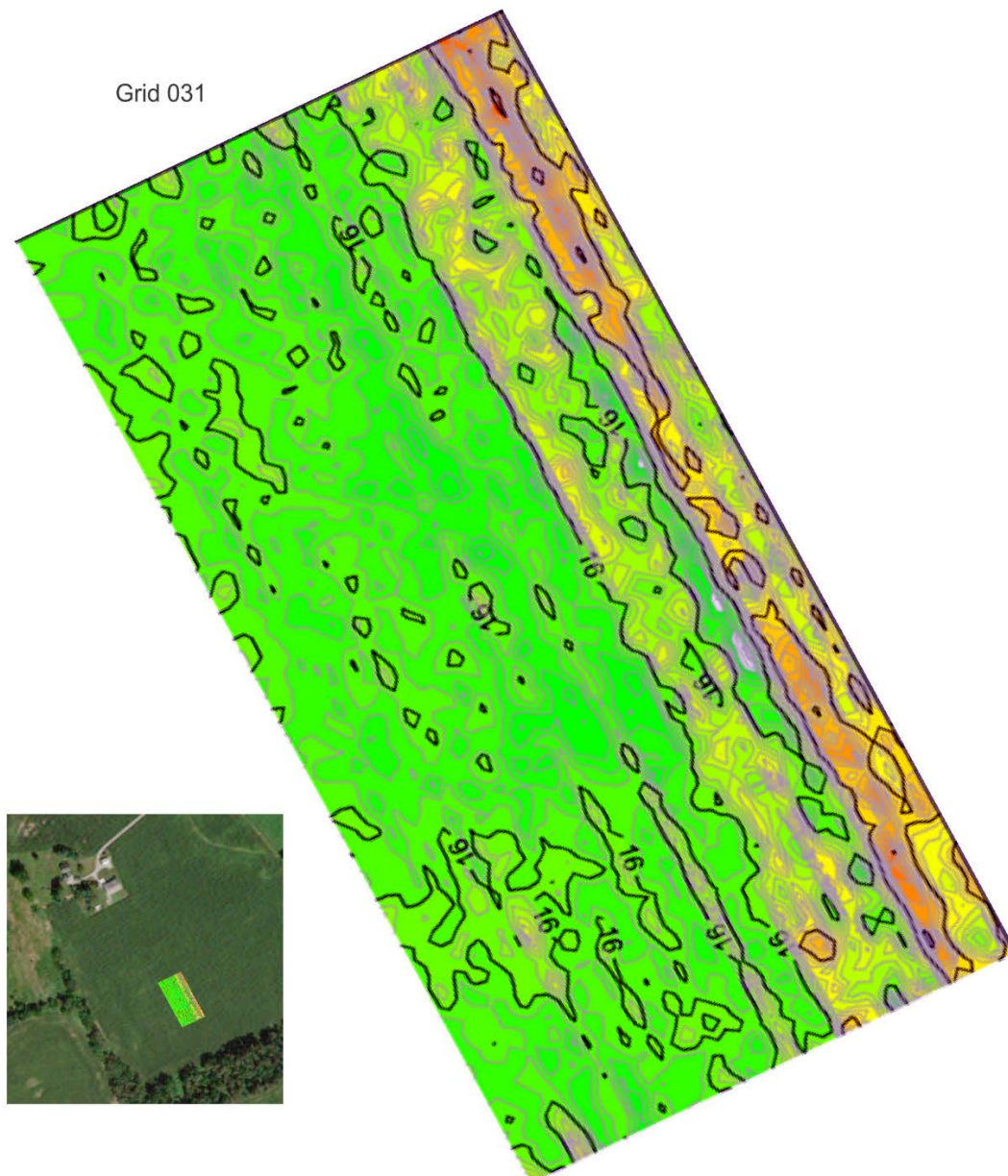


Figure 33. EM conductivity results from the Schultz block grid.

ANOMALIES OF INTEREST: HIGH RESOLUTION GPR AND EM GRIDS

Schultz Block

In both the high resolution GPR and EM data we captured eleven (11) anomalies that were of sufficient size and depth to be considered as potential targets or anomalies of interest (AOI). Within the Schultz block high resolution GPR grid we found 5 AOIs. Schultz block AOI 1 (SB-1) is a linear feature running parallel to the 470ft elevation roughly east-northeast to west-southwest, and is approximately 0.75m in depth (Figure 34, Table 3). This feature appears to end $\frac{3}{4}$ of the way across the grid to the west and extends beyond the grid to the east. SB-2 is a areal feature along the southern edge of the grid. It first appears at 0.75m and disappears at 1.5m in depth, however it is most prominent at 1.2m depth. The feature covers approximately 180m², but may extend off of the grid to the southeast. SB-3 and SB-4 are circular features which are seen most prominently at 1m depth, but extend down to 1.75m. SB-5 is a linear series of point features extending from northwest to southeast in the southern section of the grid. This set of feature is only apparent at depths between 1.2m and 1.45m and may simply represent rodent burrows, as the individual features are not a set distance from each other.

Wiest Block

Six separate AOIs were found in the Wiest block high resolution GPR and EM data (Figures 35. 36). WB1-1 appears at the surface and extends to a depth of approximately 0.75m and has been identified as a test hole TU2 from the 2015 excavation in the Wiest block. The excavated portion of this WB1-1 is clearly visible in the upper most GPR slice (0-31.9cm), but a much smaller feature located within the excavation extends deeper and may represent a rodent burrow or similar void. WB1-2 is a linear series of point features extending northwest to southeast at a depth of 0.8 – 1.25m. This feature is similar to SB-5, although the individual targets appear to be somewhat more evenly spaced. WB1-3 is a large angled feature found along the southern edge of the grid. The angle of this anomaly is approximately 90 degrees and appears to extend off of the grid. This feature is first apparent at 0.3m and extends down to a depth of approximately 2.5m, and therefore is likely geologic artifact. WB1-4 is unlike any other GPR anomalies found thus far, in that it is a large square area of highly negative GPR returns extending from approximately 0.3m to 2.25m depth, although it is most apparent between 0.5 and 1.5m. This feature may also be a geologic artifact. Anomaly WB2-1 is a linear feature most visible at the surface and appears to be soil compaction caused by heavy equipment moving across the area. Interestingly, in the same area another linear anomaly is present, but at a depth of between 0.5m and 1m. Given that this area is an access point for the Wiest field, the deeper anomaly may represent earlier heavy equipment tracks. This feature was also seen in EM grids 27 and 28. Finally, WB3-1 is a linear feature running north-northwest to south-southeast through the high resolution EM grid 22. Unfortunately this area was not covered by the GPR and we have no indication of the depth of the anomaly. This anomaly appears to extend beyond EM grid 22, however, it runs directly downslope and may simply be a filled erosion gully.

Anomaly Ranking

Based on Steve Warfel's work both at Camp Security and other colonial period sites, he has identified the stockade trench as the most likely camp related feature to have survived (Figure 37). Therefore we feel that we should give the highest rankings to linear anomalies that cannot be attributed to other causes (e.g. geology, heavy equipment).

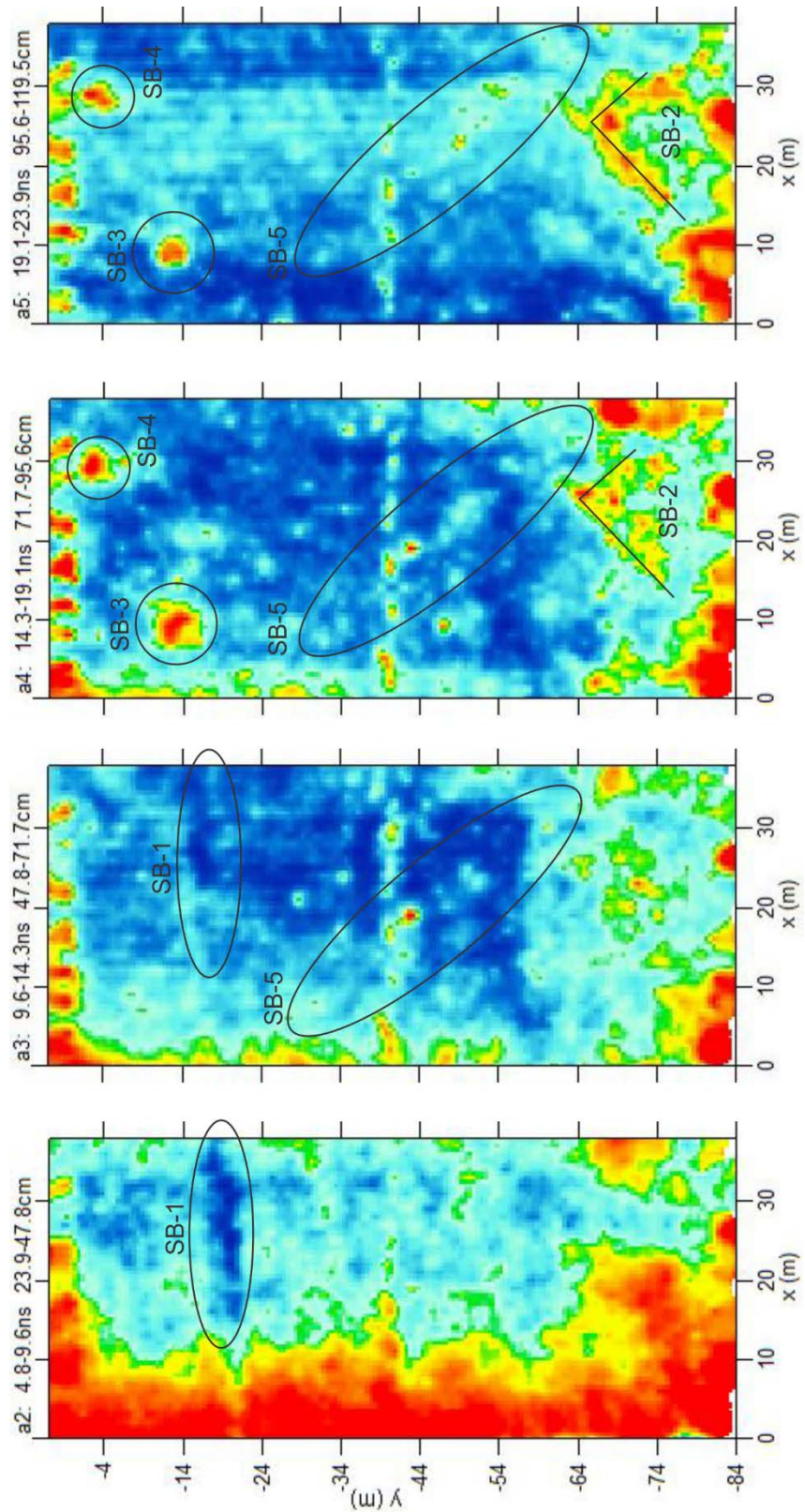


Figure 34. Shultz block GPR anomalies of interest (AOI) from the surface to $\approx 120\text{cm}$ depth.

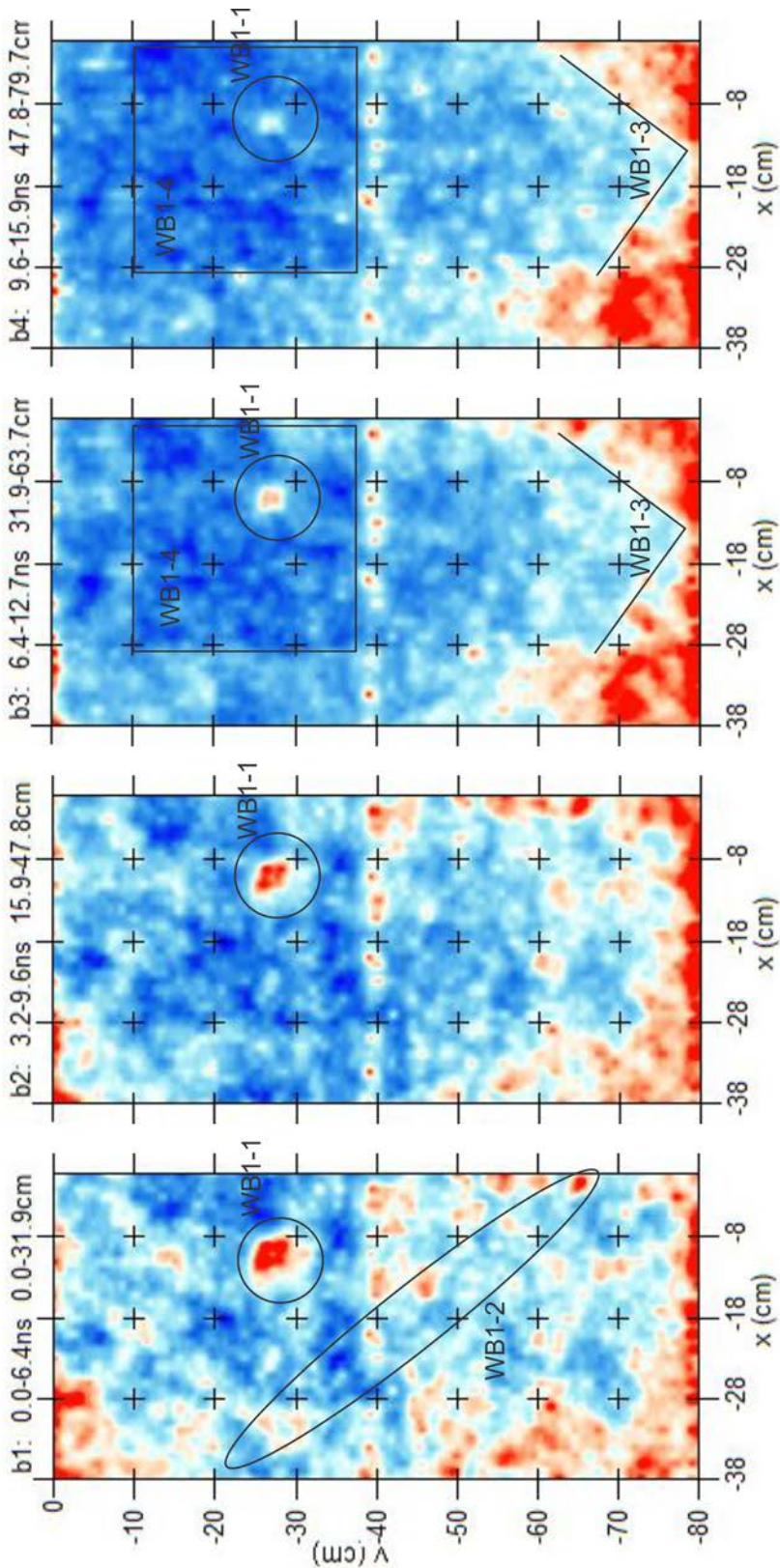


Figure 35. Wiest block GPR anomalies of interest (AOI) from the surface to ≈ 80 cm depth.

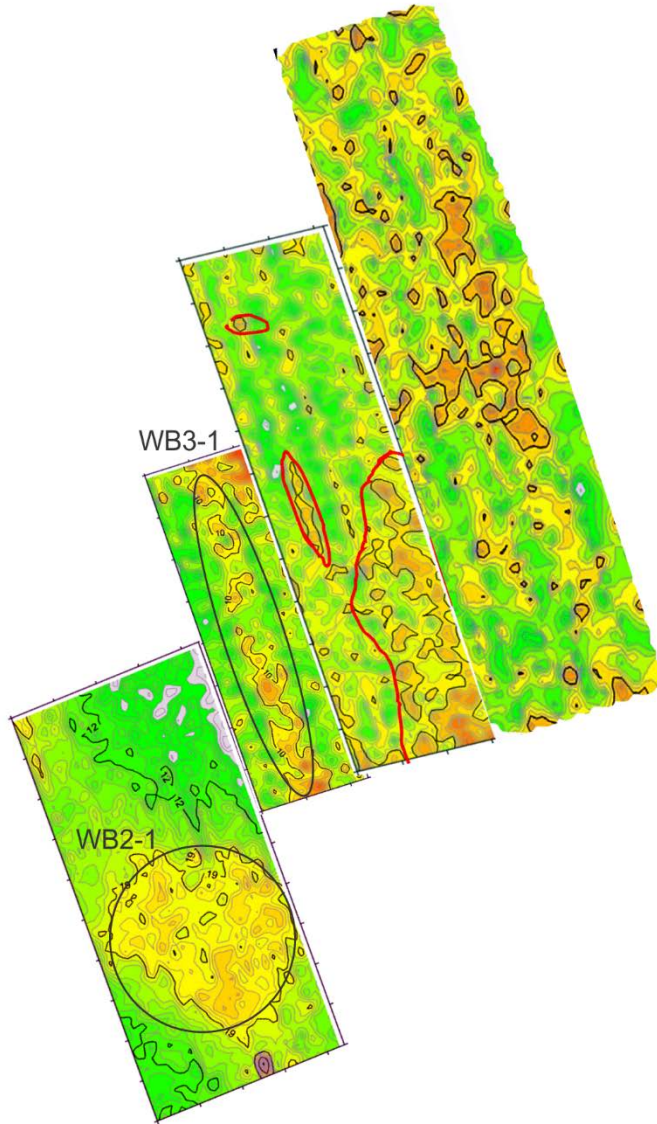


Figure 36. Wiest block EM anomalies of interest (AOI).



Figure 37. Anomalies of interest overview (also see Table 3 below).

Table 3. Anomaly ranks and locations.

ID	Coordinates*	Type	Comments	Rank
SB-1	2278501, 235617 : 2278577, 235657	Endpoints	Linear feature	1
SB-2	2278584, 235464 : 2278611, 235508 : 2278656, 235485	Angle	Angular feature	6
SB-3	2278481, 235627	Center	Deep circular feature	3
SB-4	2278529, 235682	Center	Deep circular feature	4
SB-5	2278575, 235557 : 2278651, 235525	Endpoints	Linear feature	2
WB1-1	2277726, 235103	Center	Suspected known feature	11
WB1-2	2277621, 235126 : 2277773, 234996	Endpoints	Linear feature	5
WB1-3	2277667, 234986 : 2277760, 234941 : 2277789, 235008	Angle	Angular feature	7
WB1-4	2277676, 235052 : 2277649, 235137 : 2277739, 235163 :2277765, 235082	Box	Large amorphous anomaly	8
WB2-1	2277594, 234880 : 2277592, 234763	Endpoints	Suspected known feature	10
WB3-1	2277603, 235013 : 2277649, 234585	Endpoints	Linear feature	9

*NAD_1983_StatePlane_Pennsylvania_South_FIPS_3702_Feet

RECOMMENDATIONS AND CONCLUSIONS

After eliminating known or suspected features that could be attributed to either natural processes or recent activity we have highlighted 9 anomalies that should be investigated further, and an additional 2 anomalies that we believe are *probably* not associated with Camp Security but are unusual. We tended to rank continuous linear anomalies most highly since we believe that the most likely feature we found would be a stockade trench. However, we also must mention several important points. First, both GPR and EM distinguish *differences* between reflectivity and conductivity. The more sharply defined these differences are, the more likely they will be detected. Gradual differences are very difficult to detect using these methods. We anticipated that the reflective and conductive differences between a stockade trench and the undisturbed subsoil would be abrupt and detectable by both GPR and EM. Under ideal conditions this is often the case. If portions of the stockade wall remained in the ground, our ability to detect reflective and conductive differences would be even greater. In at least 2 of the AOIs we saw strong continuous linear features that we could not attribute to natural processes, and these were ranked highest (1,2). Second, if a stockade trench was refilled with similar material as to what was removed, the reflective and conductive differences may be more subtle and difficult to distinguish in the data. Therefore, linear AOIs that we ranked lower because they were subtle and/or discontinuous may ultimately be very important. Thirdly, the 9 unknown anomalies are what we considered to be worth further examination and we felt that each should be investigated, the ranking is simply a priority given the costs of excavation and interpretation. The final 2 suspected anomalies (10,11) are likely from modern activities and do not merit further investigation, given the cost.

We have detected a number of subsurface anomalies that we believe are consistent with superficial soil disturbance including farming activities and recent soil disturbance associated with construction of the sanitary sewer, and possibly previous archeological investigations. GPR analysis has revealed features consistent with regional bedrock trends at depth. A number of features herein referred to as anomalies of interest (AOI's) are identified within the target zone that are not readily explained by natural variables. These anomalies are located mostly within the target zone and several have been prioritized as the primary targets for future archeological investigations to be completed by the Friends of Camp Security.

Acknowledgements:

A special thank you to the Friends of Camp Security, the Millersville University Archeology Department, the Geography and Earth Science Dept. at Shippensburg and the volunteers that helped make this project possible.

References

- Adams, J. K., and Goodwin, P. W. 1975. The Chickies Quartzite and some tectonic implications. *Proceedings of the Pennsylvania Academy of Science*. 49: 165-167.
- Bascom, F. and Stose, G. W. 1938. *Geology and mineral resources of the Honeybrook and Phoenixville quadrangles, Pennsylvania*. U.S. Geological Survey Bulletin 891.
- Berg, T. M., Edmunds, W. E., Geyer, A. R., Glover, A. D., Hoskins, D. M., MacLachlan, D. B., Root, S. I., Sevon, W. D., and Socolow, A. A. 1980. *Geologic map of Pennsylvania: Pennsylvania Geological Survey*. Map 1, 4th ser., scale 1:250,000, 3 sheets.
- Ganis, G. R. and Hopkins, D. 1990. The West York Block—Stratigraphic and structural setting, in Scharnberger, C.K. ed. *Carbonates, schists, and geomorphology in the vicinity of the lower reaches of the Susquehanna River*. Annual Field Conference of Pennsylvania Geologists, 55th, Lancaster, Pennsylvania, Guidebook, p.123-135.
- Gerhart, J. M., and Lazorchick, G. J. 1988. *Evaluation of the ground-water resources of the lower Susquehanna River basin, Pennsylvania and Maryland*. U.S. Geological Survey Water-Supply Paper 2284.
- Geyer, A. R. and Wilshusen, J. P. 1982. *Engineering characteristics of the rocks of Pennsylvania*. Pennsylvania Geological Survey, 4th ser., Environmental Geology Report.
- Kauffman, M. E. and Frey, E. P. 1979. Antietam sandstone ridges-exhumed barrier islands or fault-bound Blocks. *Geological Society of America Abstracts with Programs, Northeastern Section*. 11(1):18.
- LeGrand, H. E. 1988. Region 21, Piedmont and Blue Ridge, in Back, William, Rosenshein, J. S., and Seaber, P.R., eds., *Hydrogeology*. Boulder, Colo.: Geological Society of America, The Geology of North America, v. O-2, p. 201-208.
- Lloyd, O. B., Jr. and Growitz, D. J. 1977. *Ground-water resources of central and southern York County, Pennsylvania*. Pennsylvania Geological Survey, 4th ser., Water Resource Report 42, 93 p.
- Low, Dennis J., Daniel J. Hippe, and Dawna Yannacci. 2002. *Geohydrology of Southeastern Pennsylvania, Water-Resources Investigations Report 00-4166*. U. S. Geological Survey: New Cumberland, Pennsylvania.
- Lyttle, P. T. and Epstein, J. B. 1987. *Geologic map of the Newark 1 ' 2 quadrangle, New Jersey, Pennsylvania, and New York*. U.S. Geological Survey Misc. Investigations Map I-1715, scale 1:250,000.
- MacLachlan, D. B. 1990. Paleozoic carbonates of the continental margin in the Lancaster-York Valley, Pennsylvania, in Scharnberger, C. K. ed., *Carbonates, schists, and geomorphology in the vicinity of the lower reaches of the Susquehanna River*. 55th Annual Field Conference of Pennsylvania Geologists Guidebook. Lancaster, Pennsylvania. p. 116–122.
- Prowell, George R. 1907. *History of York County, Pennsylvania: Volume 1*. Chicago: J. H. Beers and Company.

Stose, G. W. and Jonas, A. I. 1923. Ordovician overlap in the Piedmont Province of Pennsylvania and Maryland. *Geological Society of America Bulletin*. 34: 507-524.

Stose, G.W., and Jonas, A.I.,1939, *Geology and mineral resources of York County, Pennsylvania*. Pennsylvania Geological Survey, 4th ser., Bulletin C 67.

Stose, A. I. J. and Stose, G. W. 1944. *Geology of the Hanover-York district, Pennsylvania*. U.S. Geological Survey Professional Paper 204.

Taylor, J. F. and Durika, N. J. 1990. Lithofacies, trilobite faunas, and correlation of the Kinzers, Ledger and Conestoga Formations in the Conestoga Valley, in Scharnberger, C. K., ed. *Carbonates, schists, and geomorphology in the vicinity of the lower reaches of the Susquehanna River*. 55th Annual Field Conference of Pennsylvania Geologists Guidebook. Lancaster, Pennsylvania. p. 136-155.

Wagner, M. E. and Srogi, L. 1987. Early Paleozoic metamorphism at two crustal levels and a tectonic model for the Pennsylvania-Delaware Piedmont. *Geological Society of America Bulletin*. 99,: 113-126.

Walcott, C. D. 1896. *The Cambrian rocks of Pennsylvania*. U. S. Geological Survey, Bulletin 134.

Appendix 0:

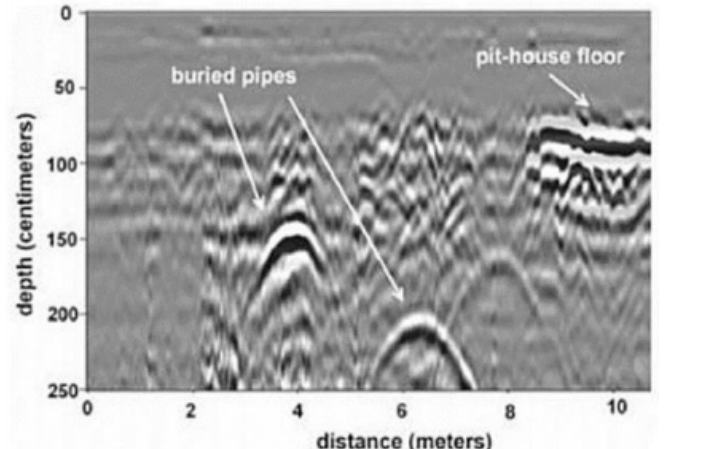
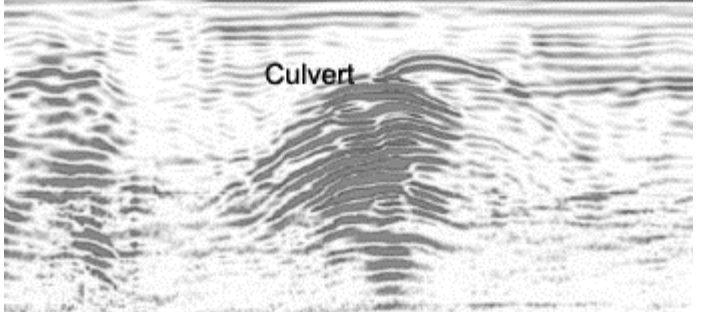
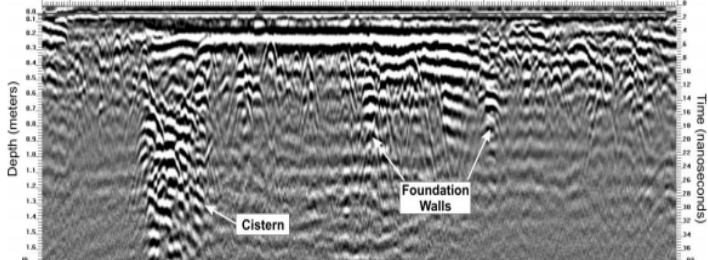
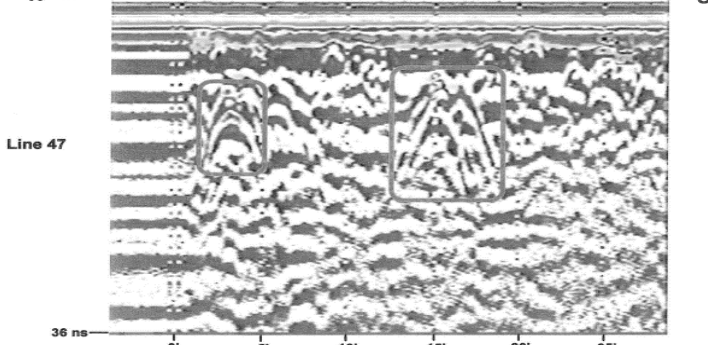
Individual radargrams for each GPR transect can be found in the accompanying document Camp Security Radargrams.pdf. For the location of specific transects, please refer to the accompanying ArcGIS 10.5 geodatabase (Camp_Security.gdb). The naming convention for the transects is SchultzGPR10mTransects for the 10 meter Schultz block GPR transect. 1m and EM transects follow the same naming convention.

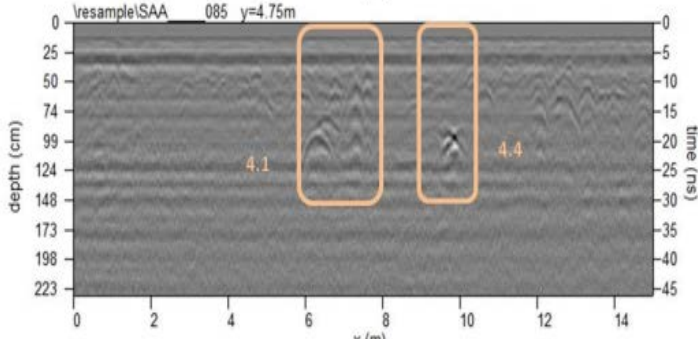
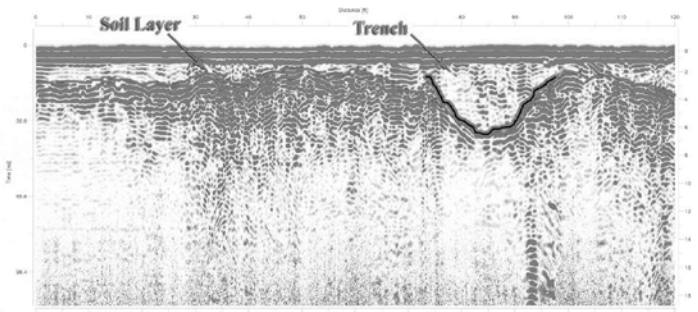
Appendix 1:

Table showing the number of anomalies identified in Schultz block radargrams by transect for the 80m x 40m grid. Categories for the anomalies are based on overall appearance of the reflectors.

Transect	Grouped	Solitary	Near Surface	Dipression
Tran 3	1	0	0	0
Tran 4	0	1	2	0
Tran 5	0	1	3	1
Tran 6	1	0	2	0
Tran 7	1	2	1	0
Tran 8	0	1	0	0
Tran 9	1	0	3	1
Tran 10	1	2	2	1
Tran 11	0	1	2	1
Tran 12	1	1	1	2
Tran 13	2	0	1	0
Tran 14	1	1	3	1
Tran 15	1	0	0	1
Tran 16	1	1	3	0
Tran 17	1	0	1	1
Tran 18	1	2	0	1
Tran 19	1	1	0	0
Tran 20	3	0	2	0
Tran 21	1	0	0	1
Tran 22	0	1	1	0
Tran 23	1	0	2	0
Tran 24	0	2	1	1
Tran 25	1	0	0	0
Tran 26	1	0	0	1
Tran 27	2	0	2	0
Tran 28	1	0	1	1
Tran 29	1	0	0	0
Tran 30	2	0	1	0
Tran 31	2	0	0	0
Tran 32	2	0	0	0
Tran 33	1	1	3	1
Tran 34	1	1	0	0
Tran 35	1	2	0	0
Tran 36	2	2	1	0
Tran 37	1	0	0	0
Tran 38	1	1	0	1
Tran 39	0	0	3	0
Tran 40	1	0	3	0
Tran 41	2	1	1	1
Sum	41	25	45	17
Percent	32.03	19.53	35.16	13.28

Appendix 2: Interpreted radargram returns from the literature

Class	Radargram Response	Interpretation	Study
hyperbolic point & planar		<ul style="list-style-type: none"> • Buried pipes • Planar pit-house floor 	Conyers, 2006
Broad hyperbolic		<ul style="list-style-type: none"> • Buried culvert 	www.geophysical.biz
Stacked hyperbolic with deep returns		<ul style="list-style-type: none"> • Filled cistern • Buried foundation 	Burks 2006
Stacked hyperbolic		<ul style="list-style-type: none"> • Graves invaded by tree roots 	

<p>Stacked hyperbolic</p>		<ul style="list-style-type: none"> • Unexcavated stockade posts (4.1) and unknown point feature 	<p>Fort Shirley (publication)</p>
<p>Patterned planar reflectors</p>		<ul style="list-style-type: none"> • Soil horizons and large-scale (25-30') buried trench 	<p>www.geoviewinc.com</p>

Appendix 3: Dielectric Permittivity of Common Materials

Material	RDP
Air	1
Dry sand	3-5
Dry silt	3-30
Ice	3-4
Asphalt	3-5
Limestone	4-8
Clay	5-40
Concrete	6
Saturated silt	10-40
Average organic-rich surface soil	12
Organic-rich agricultural land	15
Saturated sand	20-30
Fresh water	80

From: Smith, Donna Marie, 2013, Comparing the Effectiveness of Ground Penetrating Radar in Locating Stockade Features at Prehistoric and Historic Archaeological Sites, Unpublished M.A. Thesis, Indiana University of Pennsylvania, 161 p.